Interaction forces and cell sorting between two different cell types in hetero-spheroids

Kefala, Georgia-Maria

Interaction forces and cell sorting between two different cell types in hetero-spheroids

THESIS

submitted in partial fulfillment of the
requirements for the degree of

MASTER OF SCIENCE
in
PHYSICS

Author :	Georgia-Maria Kefala
Student ID :	3070573
Supervisor :	Prof.Dr. Thomas Schmidt
2^{nd} corrector :	Prof.Dr. Erik Danen

Leiden, The Netherlands, January 30, 2023

Interaction forces and cell sorting between two different cell types in hetero-spheroids

Georgia-Maria Kefala

Huygens-Kamerlingh Onnes Laboratory, Leiden University
P.O. Box 9500, 2300 RA Leiden, The Netherlands

January 30, 2023

Abstract

To better understand tumor progression and metastasis, it is important to investigate the mechanical properties of its cellular components. Tumors generally consist of cancer cells and healthy cells, whose interactions are fundamental for their structure and functionality. It has been shown that in co-cultured spheroids, cells rearrange themselves and completely separate. To closely mimic the tumor micro-environment in-vitro, hetero-spheroids containing both cancer cells and fibroblasts were used. The forces generated during cell-cell interaction and their cell sorting were studied. The interaction between the two cell types was probed with cell-sized (15-30 μm) microparticles. Different seeding-times and number ratios were investigated. No significant difference in the stress fields applied by the two different cell types during their interaction was found. However, it was observed that there is a critical number ratio between 1:3 and 1:6, above which the two cell types tend to completely separate. Below the critical ratio, there were intermixed areas of both cell lines. These cell clusters tend to merge over time, however no complete phase separation of the two cell types was observed for a period of one week. These results show that there is a favourable rearrangement of the cells consisting tumor-like structures. This cell type separation could indicate the next steps towards understanding the clustering and detachment of the cancer cells from the primary tumor, during metastasis.

Contents

Chapter 1

Introduction

The three dimensional culture of cancer cells, structures called spheroids, is a common practice for studying tumor-like systems and investigating tumor growth and progression, as well as cancer metastasis [1, 2]. Tumors, however, do not consist only of cancer cells, but are a combination of cancer and healthy cells [3]. For this reason, it as a common practice to co-culture cancer and healthy cells. The three-dimensional co-culture of different cell types are called hetero-spheroids [4]. Just like all multicellular structures, tumors rely their structure and functionality on the interactions between its cellular components [3]. Therefore, understanding the mechanical interactions between the cells forming the tumors may bring us a few steps closer into answering open questions, like how cancer progresses and metastasizes.

When two cell types intermix to form an hetero-spheroid, the interaction forces between them are important to understand how the structure forms and grows. Aside from that, another topic that has not yet been intensely studied, is the phase separation of two types of cells when they are seeded together. When two cell types are co-cultured, they are randomly intermixed. However, it has been shown from previous studies that the cells have some preferential configurations, resulting into a cell sorting [5]. The different cell types tend to cluster together, initially into small aggregates, which as the cell differentiation progresses, they merge forming bigger clusters [6]. In a simplified model, cells are resembled as active liquids. Using such model, the cell line with lower surface tension is surrounding the cell type with higher surface tension [5].

In this thesis, hetero-spheroids, formed by skin cancer (melanoma, MV3) cells and fibroblasts (SV80), were studied to investigate both their interaction forces and their mixing organization under different initial condi-

tions. The two cell types were seeded in different seeding-time conditions. A single-cell suspension of SV80 fibroblasts was added to 2-day-old melanoma MV3 spheroids or vice cersa. Different number ratio conditions between the two cell types were also used. Melanoma MV3 cells were found to divide faster than the SV80 fibroblasts. For this reason, as well as because the MV3 cells were seeded two days earlier, several ratios with increased number of fibroblasts were created. Five different number ratios ranging from 1:1-1:10 (MV3:SV80) were tested. The number of melanoma cells was kept constant at 1000 cells, while the number of fibroblasts was varied between 1000 and 10000 cells. For the investigation of the cells' interaction forces, soft hydrogel microparticles were embedded into the spheroids [7]. The three-dimentional imaging of the microparticles took place at 3 days after the start of the experiment, while the two-dimensional imaging of the entire spheroids for studying the mixing of the cell occurred 4 and 7 days after the start of the experiment.

The cells interacted with the microparticles, causing deformations of the microparticles' surface. The deformations of the microparticles' surface were translated into a stress field, by using spherical harmonics [7]. A new method was developed which distinguished the signals between the two different cell types. The method identified which cell type is found in a specific area of the microparticle's surface. Next, it assigned the stress field applied by the two cell types, by matching the stress found in the areas were a specific cell was identified. The mean values of normal and shear fields applied by both cell types were calculated. A method for investigating the mixing of the cells was also developed. The number of clusters formed by the two cell types in each of the different initial conditions, as well as the number clusters found inside a bigger group of the other stain, was quantified. This was done twice, for images taken at day 4 and at day 7 of the experiment, for the same spheroids, to identify any changes in the cells' mixing over time.

By comparing the normal and shear stress as calculated for the two cell types, no significant difference was found in the stresses MV3 and SV80 cells apply during their interaction. From the cell sorting experiments, it was found that, when using transducted MV3 and SV80 cells lines, the SV80 had a lower surface tension, since they surrounded the MV3 cells. By looking at the lower number ratio conditions (1:1, 1:3), a small decrease of the number of clusters and an increase on the average cluster-size was observed, indicating that smaller clusters may merged into larger ones. It was also found that the the ratio 1:6 is a critical ratio, above which the two cell types are almost completely separated.

It is still necessary for more data to be gathered for increased accuracy

of the analysis. The size and quality of our data may have not been large enough to conclude that during their interaction, the MV3 and SV80 cell types apply similar forces.

The mixing of MV3 and SV80 cell lines, consistently showed a phase separation above a critical ratio between 1:3 and 1:6. However, in smaller number ratios, although it was shown that smaller clusters tend to merge, no complete phase separation between the two cell types was observed in a period of one week. Further investigations should include imaging and analysis of the same spheroids for a period much longer than a week, to clearly identify whether the cells are finally sorted in the same configuration, even when they start from different seeding conditions.

Chapter 2

Theory

Hetero-spheroids are three dimensional co-cultures of two or more different cell types. In this project, skin cancer (melanoma-MV3) cells and human fibroblasts (SV80) were seeded together forming hetero-spheroids, resembling small tumor-like structures. As the spheroid grows, the cells apply certain interaction forces, which can be measured with embedding stress sensors in the structure. Apart from their interactions, another interesting question we address in this project is how mixed the two cell types are after some days of growing the spheroid. The two cell lines were randomly intermixed, but as it has been indicated before, the cells tend to sort out as the spheroid grows [5].

2.1 Stress measurements

On a cellular level, all the multicellular components, such as the skin, blood and muscles, rely their structure and function on the interactions between the cells. Likewise, tumors also rely on the junctions of cancer cells. Tumor structures do not consist only of cancer cells. Up to 50 % of the tumor may consist of other types of cells, such as fibroblasts, endothelial cells or other cellular and non-cellular components. In some cases the interaction between cancer cells with healthy cell types acts as tumor-progressive, and it is crucial for the tumor's growth [3]. By understanding these interactions, many findings can be deduced of how tumor growth and metastasis work.

For the investigation of these interactions, the method of 3D cell structures cultured in vitro, called spheroids were used. When the cells are seeded in the special wells, a spheroid is formed as the shape with the

most decreased surface tension, which makes it the most energetically favourable structure. During and after the formation of the spheroid, the cells are applying interaction forces to one another holding the structure from falling apart. These interaction forces have many ways of being measured, such as atomic force microscopy (AFM) [8] and cavitation rheology (CR) [9] techiniques. In this project, we implemented deformable microparticles [7], for measuring the cells' forces. When these particles are embedded in the spheroid, the cells interact with them and deformations on their surface appear. These deformations are a direct tool for measuring the forces the cells apply and quantify their interaction [10]. A schematic of this approach can be seen in Figure 2.1.

Melanoma cells have been classified as one of the most metastatic type of cells [11]. The main reasons for this behaviour have yet to be identified. The forces melanoma cells apply to their surrounding cells should play a key role to their migration. Therefore, by investigating the interactions of melanoma cells and fibroblasts in spheroids, it might bring us a few steps toward understanding the reasons melanoma cells are so highly metastatic.

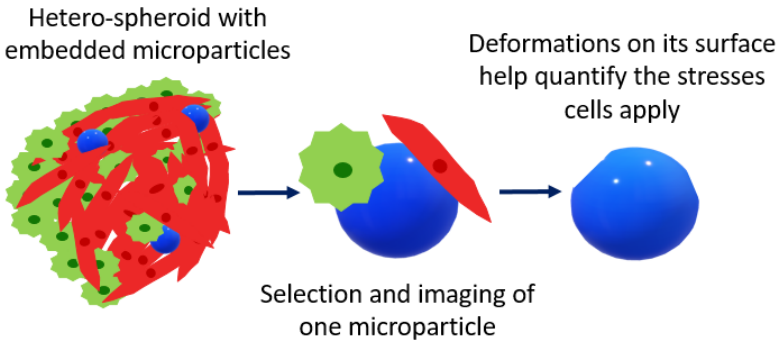

Figure 2.1: *A schematic of a spheroid with embedded soft microparticles, acting as stress sensors. The cells in a spheroid interact with one another and with the microparticles. By analysing the deformations in their surface, the stresses the cells apply can be identified.*

2.2 Phase separation

Even though two different cell types, when seeded together, they randomly intermix, the resulted spheroids might show cell sorting. Such properties have been investigated before, in which studies the cells are being treated as liquid, with their surface tension being the quantity of importance. It has been shown that the cell type with lower surface tension surrounds the cell type with higher surface tension [5, 12].

Previous studies have shown a series of effects when different cell types are intermixed [6]. These effects include the most recurring phenomenon, that of the cell type with the lowest surface tension to surround the other one, but also that of small subgroups of cells to merge into larger clusters, as well as the rearrangement of the cells to the same final configurations even when different initial conditions are followed. During the latter, the cells rearrange themselves in the structure until the most stable configuration is achieved [5].

The case where a system, consisting of two or more different components, is built having an unstable initial stage, after which the system undergoes a phase transition, is called spinodal decomposition [13]. This phenomenon was first studied in glasses, and it was fast expanded on polymer and liquid solutions studies. Spinodal decomposition is a counter-intuitive phenomenon, since it does not obey the second law of thermodynamics. The system from a uniformly mixing state, where all the components are completely intermixed, spontaneously relaxes into a state where its components have been completely separated. The system tends to relax on a more ordered state. [13]. Former studies performed in solids, showed that when the two mixed compounds differ significantly (e.g. their chemical composition is different), then they tend to undergo a phase separation [14]. Likewise, the biological differences between cancer cells and fibroblasts may be large enough for a three-dimensional living system consisting of these two type of cells to obey this phenomenon. In any case, spontaneous phase separation of two cell types, even after they were randomly intermixed, has been observed before [5, 15].

With this knowledge, we investigated the mixing of melanoma MV3 and SV80 fibroblasts cell lines, under different conditions. The most studied condition in literature is the one where both cell types are seeded together at the same time, which immediately shows evidence as to which cell type is the one with the higher and lower surface tension. By seeding one of the cell types first and then adding the other in different cell amounts, different initial mixing conditions may apply. The mixing stops being random, since the second cell type is seeded into an already formed

spherical structure consisted of the first cell type. By performing this experiment, it is possible to track the mixing of the two cell types under different conditions and to investigate if the cells will follow a complete phase separation after a span of some days, as indicated by former studies [6]. In Figure 2.2, a schematic of the random seeding process, which finally leads to the cell type with the lower surface tension being spread around the other cell type, is being shown.

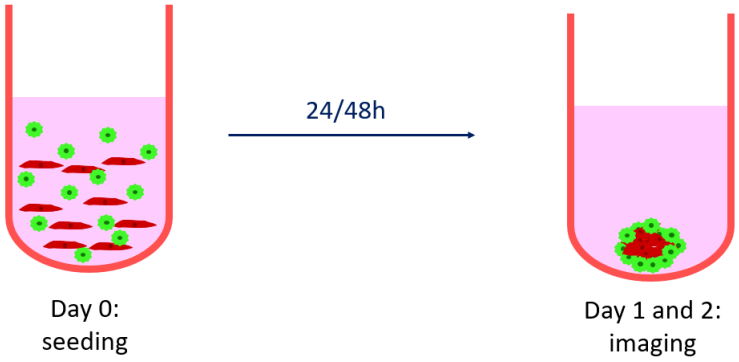

Figure 2.2: *A schematic of the random mixing of cells which leads to the spreading of the cell type with the lower surface tension around the other cell type.*

Chapter 3

Materials and Methods

To study the forces and phase separation in co-cultured spheroids, melanoma MV3 cells and SV80 fibroblasts were used. The cells, after performing staining, were seeded in different conditions for forming spheroids. Soft microparticles were embedded in the spheroids, which served as stress sensors. The spheroids were imaged with a Spinning Disk Confocal Microscope, and two methods were developed for analysing the obtained images. The first method distinguished between the two cell types for identifying the stress field each one applies. With the second method an image analysis on a two-dimensional scale was performed for investigating the phase separation of the cell types for different seeding conditions.

3.1 Cell culture

MV3 (melanoma cells) and SV80 (fibroblasts) cells were cultured in Dulbecco's Modified Eagle's Medium (DMEM, Gibco, 11965092), supplemented with 4 mM L-glutamine, 100 $\mu g\ mL^{-1}$ penicillin/ streptomycin and 10 % Fetal Calf Serum. The cells were typically split twice per week, in ratios 1:10 for the MV3 and 1:5 for the SV80 and incubated in 37^{o}C with 5 % CO_2.

3.2 Spining Disk Confocal Microscope

For imaging of the spheroids, a home-build spinning disk confocal high-resolution microscope was used. The set up consisted of an Axiovert 200 (Zeiss) inverted microscope and a CSU-X1 (Yokokawa) spinning disk unit. A 40x oil objective with NA of 1.30 was used for the three-dimensional imaging of the microparticles inside the spheroids, while a 10x objective

with NA of 0.20 was used for studying the mixing of the cell types. The images were acquired with an emCCD camera (Andor, iXon DU897). The lasers used according to the staining type were the following:

1. 405 nm (CrystaLaser): Hoechst
2. 488 nm (Coherent): CellMask Green, LifeAct YFP, LifeAct EGFP
3. 561 nm (Cobolt): CellMask Orange, CellTracker Orange, LifeAct mCherry
4. 642 nm (Spectra): CellTracker Deep Red, Alexa-647 Cadaverin

3.3 Cell staining

Fluorescent microscopy was used to obtain high resolution images of the MV3 and SV80 cell's position and structure, for investigating their forces and mixing when seeded together. For this, different kinds of life-cell staining were tested, to investigate the interactions and mixing of the two cell types as the spheroid grew.

3.3.1 CellMask

Initially, CellMask Green (ThermoFisher, C37608) and Orange (ThermoFisher, C10045) were used for staining of the MV3 and SV80 cell lines respectively. The effectiveness of these membrane dyes were tested in two-dimensional monolayers as well as in three-dimensional systems.

For the two-dimensional case, both MV3 and SV80 were seeded separately in an an imaging dish (Ibidi, 80136) in 1:5 concentration. 0.1 % v/v final concentration of CellMask Orange and CellMask Green was added. After 1 hour of incubation, the cells were washed. Given that we need a staining stable enough to give clear signal of the cells' position and structure for at least 7 days, to be able to study the changes in the mixing and the interactions between the two cell types using image analysis, the effect of the dyes was tested days after their staining. Figures 3.1(a-d) show the same samples of the two cell types as imaged right after washing and 24 hours later. In this images, Hoechst (ThermoFisher, 62249) was also used for staining the nucleus of the cells. This was performed by adding 1 $\mu g\ mL^{-1}$ final concentration of Hoechst and incubating for 10 minutes before washing.

From these results, it is evident that the membrane staining with CellMask was not sufficiently stable to obtain a clear signal for a long period of time.

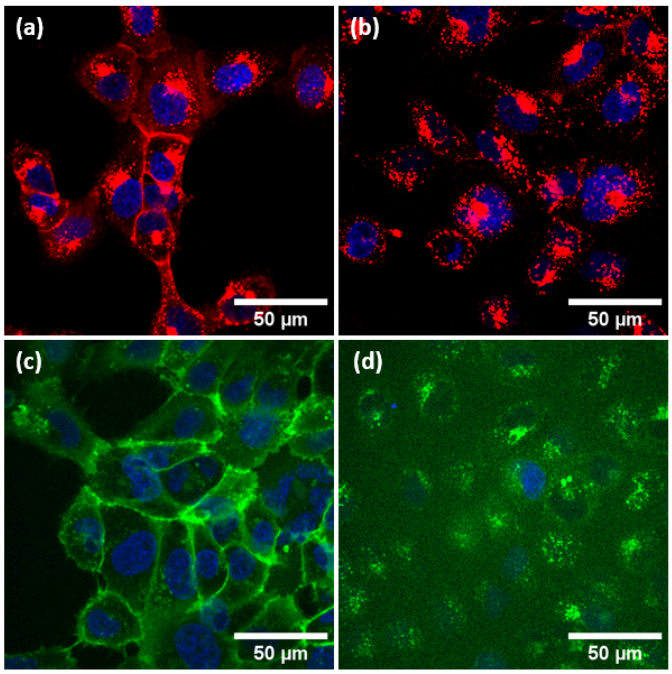

Figure 3.1: Results of the CellMask staining. ***(a)*** *SV80 with CellMask Orange, imaged right after the end of the staining process and* ***(b)*** *after 24 hours.* ***(c)*** *MV3 with CellMask Green right after the end of the staining process and* ***(d)*** *after 24 hours.*

3.3.2 CellTracker

Since staining the membrane of the cells did not give the desired results, a cytoskeleton staining was also tried, by using CellTracker Orange (ThermoFisher, C34551) and DeepRed (Thermofisher, C34565) for the MV3 and SV80 cell lines respectively. The dyes were added in the cell medium in 1 μM final concentration and incubated for 30 minutes before washing. Figure 3.2 shows the results for this type of staining, right after the incubation as well as after 24 hours.

Staining with CellTracker was proved more stable over time than that of the CellMask. However, the obtained signal was still not sufficient to perform detailed image analysis for finding their position on the particle's surface and their mixing compositions.

3.3.3 Transduction

To improve the signal to noise, we used transduction. All the previous staining methods did not allow the detailed analysis of the cells position

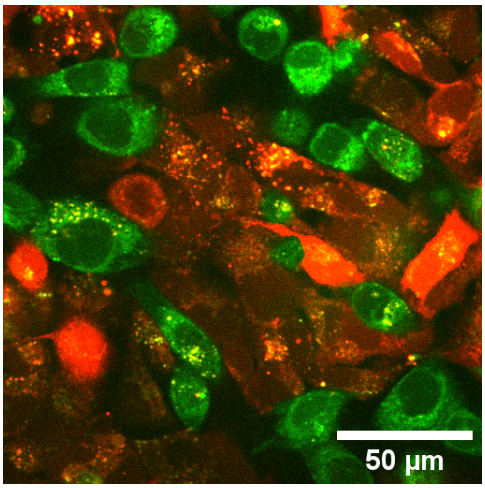

Figure 3.2: *SV80 (red) and MV3 (green) cell lines stained with CellTracker DeepRed and Orange respectively as imaged by the Spinning Disk Confocal Microscope.*

in the spheroids, since their signal was not stable over long periods of time. Using this method, the cells expressed fluorescence without relying on external staining. Since, in this case, the fluorescence is encoded in the cells' genes, the signal is stable for long periods of time.

Transfection [16] is a method used to introduce foreign genetic material into live cells, for the purpose of expressing genes of interest, while transduction is specifically using viral DNA to make this happen. We used transduction to make our cells fluorescent by inducing the expression of two fluorescent proteins: Lifeact-EGFP (enhanced green fluorescent protein) and Lifeact-mCherry.

Lifeact-EGFP (displayed as green) and Lifeact-mCherry (displayed here as yellow), as well as a selection marker for antibiotic resistence (puromyicin) were provided through a plasmid into a culture of HEK 293 T cells. HEK 293 T served as packaging cells and produced the viruses needed for the transduction of our host cells: melanoma cells (MV3) and fibroblasts (SV80). For this purpose, three additional plasmids containing structural and regulatory viral genes were supplied in the growth medium. Once formed, the viral particles were freed into the supernatant, which was then collected and used to transduct the MV3 with Lifeact-EGFP and the SV80 with Lifeact-mCherry. A the end of the process, the positive cells were selected with puromycin.

In Figure 3.3, the transducted cell lines, as well as their wild type counterparts are displayed. The phase-contrast images were taken with a Phase

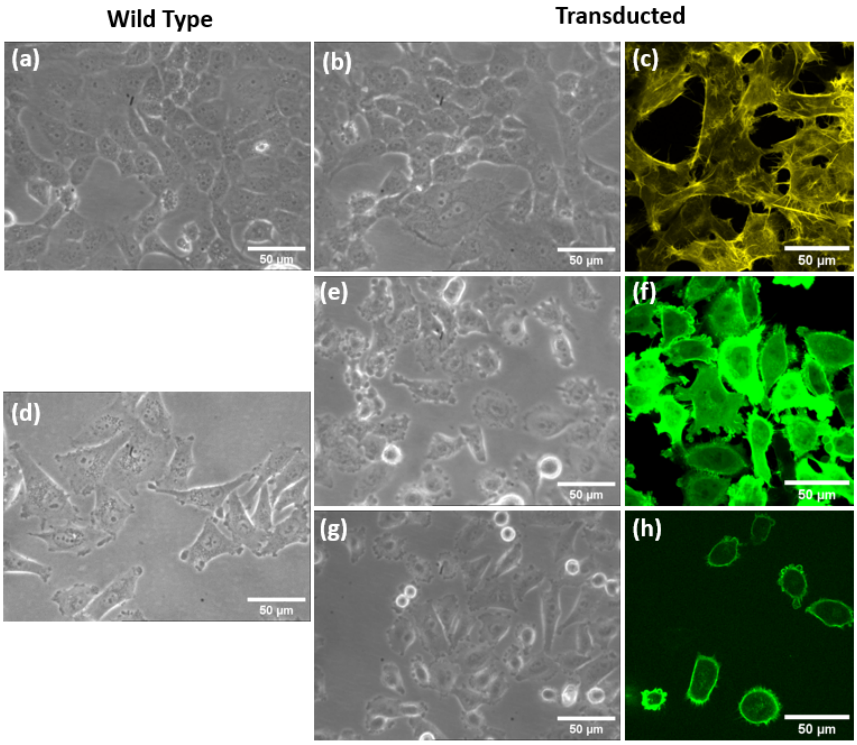

Figure 3.3: Displaying of the SV80 and MV3 wild type and transducted cell lines. ***(a)*** *SV80 wild type cells.* ***(b-c)*** *Phase contrast and fluorescent image of transducted SV80 cells expressing mCherry LifeAct.* ***(d)*** *MV3 wild type cells.* ***(e-f)*** *Phase contrast and fluorescent image of transducted MV3 cells expressing eGFP LifeAct.* ***(g-h)*** *Phase contrast and fluorescent image of transducted MV3 cells expressing YFP LifeAct.*

Contrast Microscope using a 40x objective, while the fluorescent images were taken with the Spining Disk Confocal Microscope, using a 40x oil objective. These images were acquired more than one month after the transduction was performed. It can be seen that the transduction of the cells did not alter their fundamental behaviour, such as growth, size and migration abilities, significantly when compared to their wild type counterpart. By looking at the fluorescent images, the transduction was successful, with most cells in the sample expressing the fluorescent protein of choice.

3.4 Spheroids

The main aim was to study the interaction forces of the two cell types, as well as their configuration when co-cultured in free three-dimensional structures resembling small tumors. Therefore, hetero-spheroids were produced using 96-well plates with round bottoms. The wells were treated with anti-adherence solution (STEMCELL, 07010), so that the cells do not stick on the bottom or edges of the wells and are free to form a three-dimensional structure by only attaching to each other. After performing the staining of choice and after washing with PBS, 0.5 μL of TryPsin solution (PBS+EDTA with added 25 $mg\ mL^{-1}$ TryPsin) was added so that the cells detach from the flask's bottom and were able to be transferred to tubes. The cells were resuspended in medium and were counted using an automatic counting machine. After washing the well-plate with cell medium, different cell amounts in the range of 1000-10000 cells per well were seeded, corresponding to the different conditions of interest. On top of the different seeding amounts, the conditions also differed in the seeding time of the two types of cells. An overview of these conditions can be seen below, as well as in the schematic of Figure 3.4:

1. Day 0: seeding 1000 cells of both MV3 and SV80
2. Day 0: seeding of SV80, day 2: seeding of MV3
3. Day 0: seeding of 1000 MV3, day 2: seeding of SV80 in a range of 1000-10000 cells

To measure the stresses applied by the cells, soft hydrogel microparticles serving as stress sensors were added in the cell solution. In each well approximately 15 microparticles were embedded.

3.5 Preparation of the microparticles

Soft hydrogel microparticles, mostly made from acrylamide, were used as stress sensors for identifying the stress applied from the cells [7]. Their production was a part of a previous work performed in the lab. Prior to their use in the experiments, the microparticles were functionalized and labelled.

The microparticles had a size dependent Young's modulus $Y[Pa] = 1000 * 14.842/(R_0^{1.1})$, where R_0 the specific particle's radius [7, 17]. Initially, 100 μL of the particles' stock solution, containing 15 % v/v particles

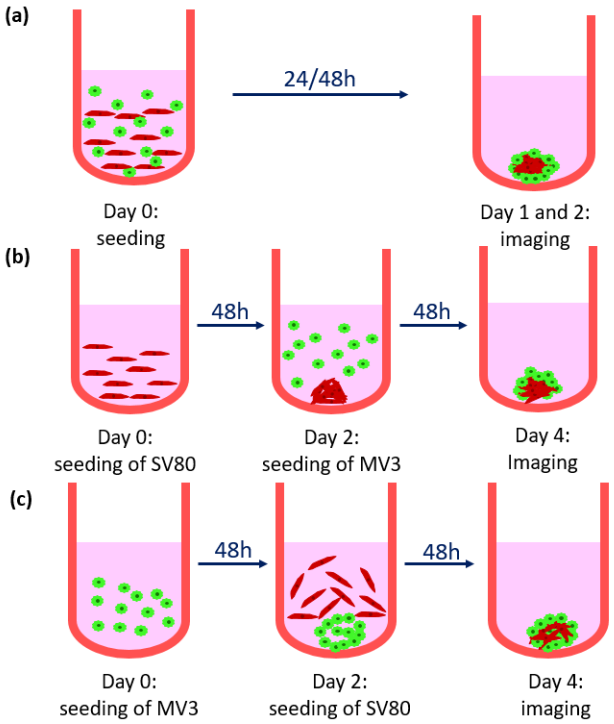

Figure 3.4: A schematic overview of the seeding conditions used to investigate the mixing of the two cell types under different initial conditions. ***(a)*** *Seeding of both cell types at day 0 and imaging at day 1 or 2.* ***(b)*** *Seeding of SV80 cells at day0 and of MV3 cells at day 2. Imaging took place at day 4.* ***(c)*** *Seeding of MV3 cells at day 0 and of SV80 cells at day 2. Imaging took place at day 4.*

in PBS, was washed twice in 0.25 % activation buffer. The activation buffer contained 100 mM MES (sodium salt) pH 6.0 and 200 mM NaCl. 2 % (w/v) NHS (ThermoFisher, 24500), 4 % (w/v) EDC (Sigma, E7750) and 0.1 % final concentration of tween 20 were added to the particle solution, to free up their reactive groups so that the protein of choice could bind to their surface. The solution was mixed and incubated for 15 minutes in room temperature. After the incubation, the solution was washed three times using PBS pH 8 + 0.1 % tween 20. A final concentration of 5 $\mu g\ mL^{-1}$ BSA was added to the solution, which was then incubated for one hour. The protein coated the particles' surface, serving as an adhering agent for cells to get attached and interact with them. The dye of choice was added, in this case 1 μL of AlexaFluor-647 Cadaverin for a final concentration of 10 μM, and the particles were incubated for 30 minutes. 100 μM final concentration of Tris-ethanolamine was added to block the NHS groups to which BSA and the Cadaverin did not bind, and incubated for 30 more minutes. The

solution was then washed three times, resuspended in PBS pH 7.4 and 1 % (v/v) sodium aside for 5 mM final concentration was added for disinfection. The microparticles were stored in the fridge and were used for the experiments up to a month after their fuctionalization.

In Figure 3.5, a sample prepared from the microparticle used for the experiments is shown, as imaged by the Spinning Disk Confocal Microscope, using a 10x objective. The Cadaverin dye homogeneously labelled the particle volume.

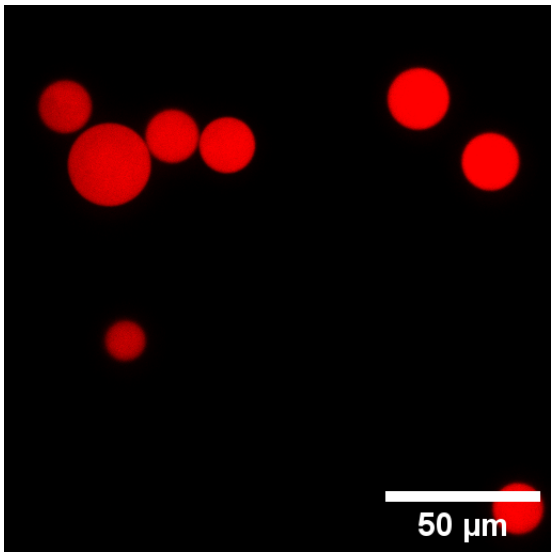

Figure 3.5: *A sample of the hydrogel microparticles used as stress sensors.*

3.6 Analysis

For the analysis of the data, two methods in MATLAB (2017a) were produced, one for each of the two experiments: calculation of the stresses each cell line (MV3 and SV80) applies and the 2D investigation of the mixing of the two cell lines.

3.6.1 Distinguishing the two cell types on the microparticle surface

After performing the already developed methods from the lab for the reconstruction and analysis of the microparticle, the stress field and the signal of the stains around the particles' edge were collected. The stress

field applied on the particle was found by looking at the deformations on its surface and using spherical harmnonics, a method first developed by Vorselen *et al.* [7] and then expanded by the lab. For the identification of which cells were touching the microparticle, a mask of size 1 μm from its edge was used. Then lines starting from the particles' center were drawn. The mean and standard deviation of the signal from every stain channel that appeared in every line and only inside the mask were obtained.

To be able to quantitatively compare the different signals coming from the different cell types, a rescaling was necessary. The stain's signals were rescaled by subtracting the background from each distribution and then dividing by the noise coming from this signal, as shown in equation (I).

$$S = \frac{S_o - bkg}{noise}(I)$$

For the calculation of the background, a mask equivalent to a sphere with radius equal to 60 % of the microparticle's radius was created and used to collect the signal appearing in the microparticles' bulk. Since cells cannot invade into the microparticle, these data correspond to pure background. In case the indentations are large and the mask does not exclude the signal coming from the edge of the particle, the background is calculated as the largest value of the 95 % of the data. The noise was identified as the standard deviation of the background data. In this way, the ability of comparing the different signals coming from the different cell types was achieved. Simulated data were made to test the method. In Figure 3.6, an example of the rescaling of the signal of the simulated data can be seen. After performing the rescaling, the background peaks are found overlapping below zero, while the signals appearing positive is the one coming from a cell that is attached to the microparticle's surface.

For the reason that the background was defined as the largest value of the 95 % of the data, the signal on the particle's surface may be overestimated and 5 % of the signal identified on its surface to be background. A condition was made that if a stain occupied 5 % or less than the overall surface area of the particle, then no cell was near the particles' edge.

Each stain signal was then compared to the other one appearing in the system. For each pixel of the particle surface, the dominant signal was determined. If this value was below 0, it was not allocated to either cell type, it was considered as background. This allocation was used to collect the normal and shear stress data corresponding to the specific stain, from which the distributions were displayed and their mean along with its standard deviation was calculated. The total mean of the stresses coming separately from the MV3 and the SV80 were compared to identify any possible difference between them. The final data returned by the method, for

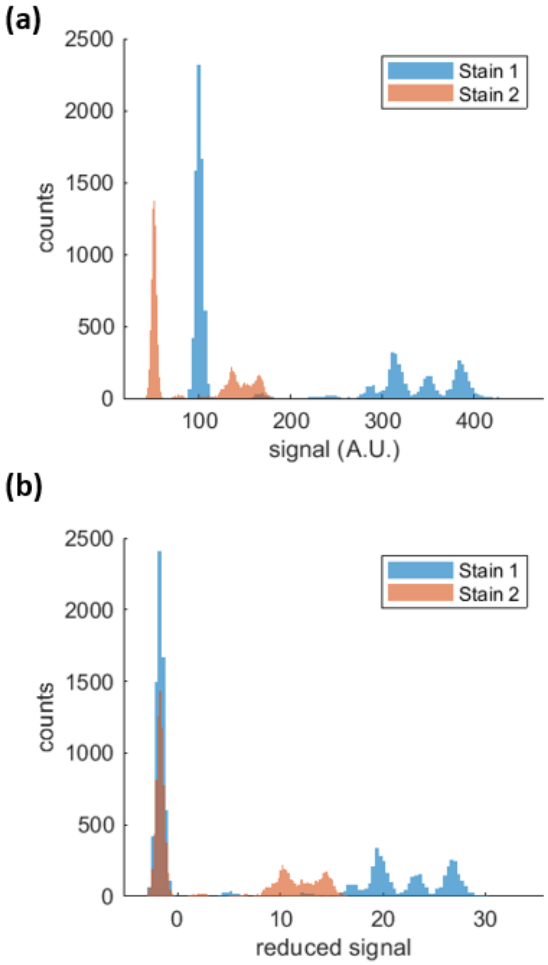

Figure 3.6: *Histogram of the* ***(a)*** *raw and* ***(b)*** *rescaled intensities of the two signals coming from the simulated data resembling a system with two stains as returned by the developed method. By performing this rescaling, the signals of the two stains become comparable.*

a set of simulation data resembling two stains on the particle's surface, can be seen in Figure 3.7. Figure 3.7(a) shows the reduced signal of the the first stain, in 3D and 2D. Right below it, the binary signal showing the position of the corresponding cell type on the microparticle's surface is displayed. The white area is where the cell was found, while the darker areas correspond to background. Figure 3.7(b) shows the same, ut for the second stain found interacting with the microparticle. Figures 3.7(c-d) show the normal and shear stress distributions, as they were assigned for each cell

type individually.

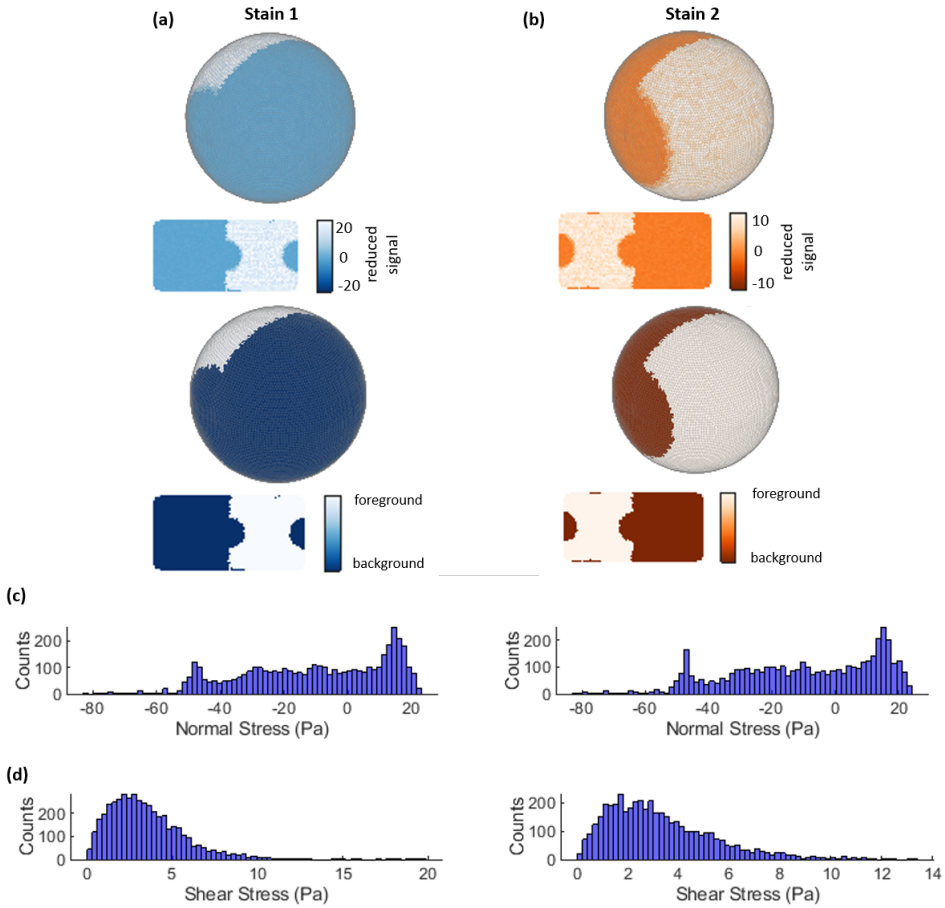

Figure 3.7: The results the developed method returned for a simulation data of two stains. ***(a)*** *Position of the first stain on the microparticle's surface.* ***(b)*** *Position of the second stain on the microparticle's surface.* ***(c)*** *The normal stress applied on the microparticle's surface by the first and second cell type, respectively.* ***(d)*** *The shear stress applied by the first and second cell type, respectively.*

3.6.2 Investigation of the cell lines' phase separation

A novel approach was developed that intended to study how mixed the two cell lines tend to be when seeded together under different conditions. This method reads the initial image and for each stain, build-in MATLAB functions were used for obtaining the mixing of the MV3 and SV80 cell types. In the biggest part of this project, we used stacks around a plane just below the middle one of the spheroid and performed calculations on

the maximum projection of the stack. To obtain the stacks, 6 images were taken in a cube of approximately 700 x 700 x 8 μm^3. The maximum projection of the stacks for each stain was then found and used as a single image. This was done for improvement of the signal obtained by the cells. Each stain was blurred by using a gaussian filter. An adaptive threshold was set, by selecting a large neighbour box around each pixel. The image was then binarized and the groups of pixels smaller than the size of a pair of cells (40 μm) were discarded, as too small cell patches which may come from image artifacts. Finally, any possible holes in the image were filled for obtaining a complete filled patch from each stain. The number of patches as well as their boundaries and areas coming from each stain were found. The method then identified whether a patch of one stain is found inside a patch of a different stain by comparing their overlap areas. If the overlap area of two patches is larger than half of the total area of the smaller patch, then the smaller patch is inside the larger one. Finally, statistics on the circularity of the patches and the average area they occupy were also obtained. This method was performed and gave statistics for all the different seeding conditions. As an example, two different spheroids analyzed by this method are displayed in Figure 3.8. In Figure 3.8(a), a spheroid formed by MV3 and SV80 cell lines which showed a complete phase separation is shown. Its seeding conditions were the number ratio 1:10, with the MV3 having been seeded at day 0 and the SV80 at day 2 of the experiment. Two patches for each of the two stains was identified. The area of the MV3 patches was calculated as $1.91x10^5$ μm^2 and $0.02x10^5$ μm^2. The area of the two SV80 patches was calculated as $1.5427x10^5$ μm^2 and $0.29x10^5$ μm^2. In Figure 3.8(b), a spheroid with SV80 clusters (red) found inside a large area of MV3 (green) is shown. The method identified 7 different SV80 patches with areas $0.12x10^5$ μm^2, $0.03x10^5$ μm^2, $0.12x10^5$ μm^2, $0.44x10^5$ μm^2, $0.27x10^5$ μm^2 and $0.03x10^5$ μm^2. The area of the MV3 spheroid was calculated as $2.28x10^5$ μm^2. The cells were seeded in the ratio condition 1:1, with the MV3 having been seeded at day 0 and the SV80 at day 2. The sketches on the right side of the figure correspond to the boundaries of the two stains' patches, displayed in μm, as found by the developed method.

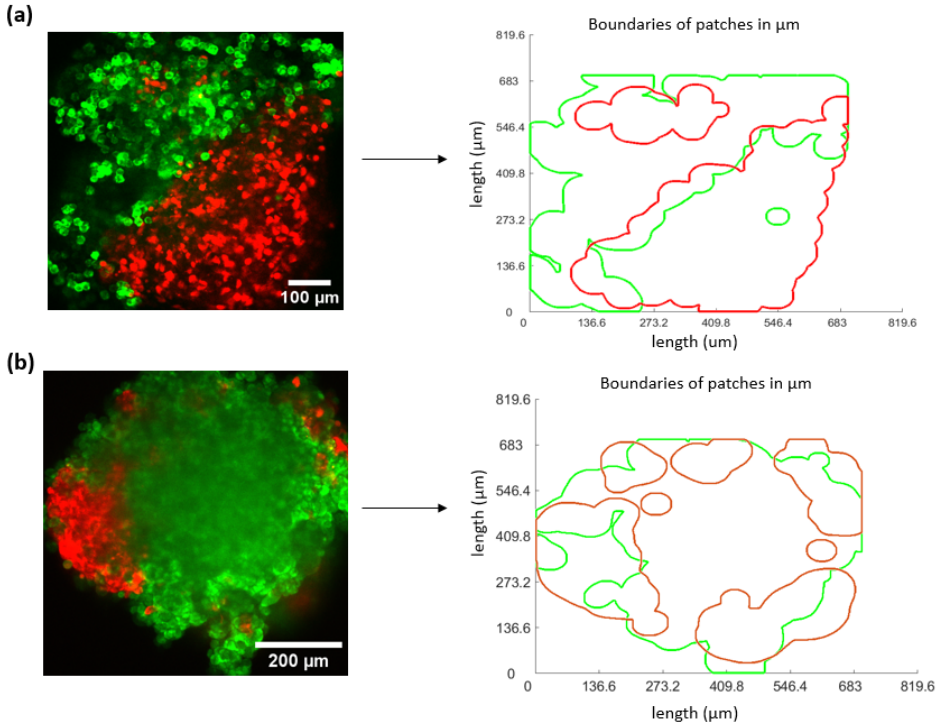

Figure 3.8: Two examples of the identification of the patches by the developed method. ***(a)*** *A spheroid showing a complete phase separation between the two cell types.* ***(b)*** *A spheroid with patches of one cell type being found inside a spherical structure formed by the other cell type.*

Chapter 4

Results and Discussion

Melanoma (MV3) and fibroblasts (SV80) were co-cultured in spheroids, for the investigation of the forces they generate as well as studying their phase separation. Soft microparticles were embedded into the spheroids, which acted as stress sensors for the quantification of the cells' interaction forces. The microparticles were imaged in three-dimensional stacks. For studying the mixing of the two cell types, different seeding conditions were used and the spheroids were imaged twice in a duration of a week. The two analysis methods described in the Methods section were used to investigate these two questions.

4.1 Distinguishing the two cell types on the microparticle surface

Two cell types, melanoma MV3 cells and SV80 fibroblasts, were seeded on a 96-well plate for the formation of spheroids. The two cell lines were transducted, expressing eGFP (MV3) and mCherry (SV80) LifeAct. The cells were seeded in different conditions, as it is summarized in the schematics of Figure 4.1. Figure 4.1(a) shows the timeline of the experiment. The MV3 eGFP cells were seeded at day 0, while the SV80 mCherry LifeAct cells were added at day 2 of the experiment. Microparticles were added at both seeding times, to maximize the possibility to find one interacting with both types of cells. The imaging of the microparticles inside the spheroids took place at day 3.

In Figure 4.1(b) the 96-well plate with the different seeding conditions is being depicted. In the first 5 rows (Figure 4.1(b), rows A-E), only 1000 MV3 cells were seeded at day 0. After 2 days (day 2 of the experiment)

the SV80 cells were seeded in these first 5 conditions in different amounts. In row A, 1000 SV80 cells were added to the pre-seeded 1000 MV3 cells, resulting in the cell number ratio 1:1 (MV3:SV80). In rows B, C, D and E, 3000, 6000, 8000 and 10000 SV80 cells were added respectively, resulting in ratios 1:3, 1:6, 1:8 and 1:10. In each well, approximately 15 microparticles were also added. In the last three rows of the plate, 1000 MV3 and 1000 SV80 were seeded at day 0 of the experiment separately (Figure 4.1(b), rows F-G) and together (Figure 4.1(b), row H), conditions which served as the controls for the specific experiment. These three control conditions allowed us to examine if the cells were behaving in a similar way in all the different repeats of the experiment.

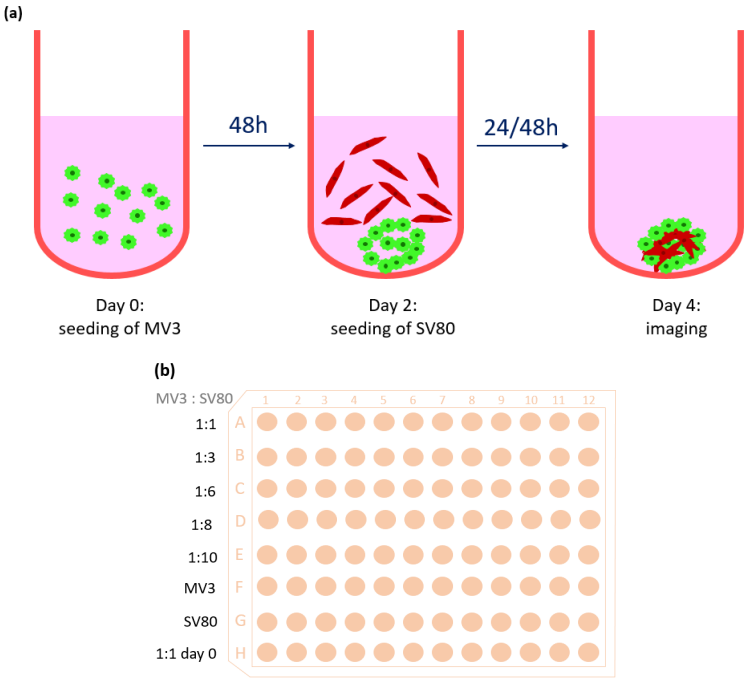

Figure 4.1: Schematic of the experiment timeline and conditions used for the identification of the stresses applied by two different cell lines. ***(a)*** *The timeline of the experiment, showing at which day each cell type was seeded.* ***(b)*** *The 96-well plate in which the two cell types were seeded, in conditions varying from 1:1 to 1:10.*

The spheroids were imaged at day 3 of the experiment. To prevent image distortions from the round-bottom culture wells, the spheroids were transferred in an imaging slide with flat-bottomed-wells (Ibidi, 81816). Using a 40x objective, stacks of microparticles were taken, in a cube of approximately 175 x 175 x 50 μm^3. The experiment was repeated 3 times,

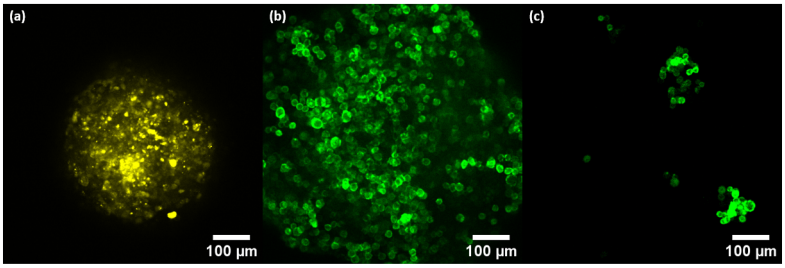

Figure 4.2: Images of the spheroids taken 4 days after the beginning of the experiment. ***(a)*** *Spheroid consisting only of SV80 cells.* ***(b)*** *Spheroid consisting only of MV3 cells.* ***(c)*** *Detached MV3 cells during the spheroid transferring from the seeding plate to the imaging slide.*

with approximately 30-40 microparticles imaged each time, found in any of the first 5 conditions.

The spheroids formed entirely out of the SV80 cells were a lot more compact, with mean diameter approximately $290 \pm 4.08\ \mu m$, than those formed only by the MV3 cells, which formed a less spherical spheroid of approximate diameter $600\ \mu m$. The MV3 spheroids, in most cases, were slightly expanding over the field of view ($\sim$600 μm). This can be seen in Figure 4.2(a-b). In both cases, 1000 cells were seeded for the formation of the spheroids. We know from cell culture that the MV3 cells divide twice as fast as the SV80 cells. Taking this into account, an MV3 spheroid should be twice the size of an SV80 one, something that seems to be obeyed. Furthermore, during the transferring of the spheroids from the seeding plate to the imaging slide, groups of MV3 cells were getting detached from the original structure (Figure 4.2(c)). During one of the experiments, the MV3-only spheroids that hadn't been transferred to be used for imaging, were gathered and the alive cells were counted. This test showed about 85% of the cell population was alive. Given that the MV3 cell islands that were detached were large (more than 100 μm), they contained living cells, excluding the possibility of them getting detached due to their death. These results show the fact that the melanoma (MV3) cells, as many cancer cell lines, exhibit loss of cell-cell adhesion [18]. They do not form very stiff connections with each other, their interactions are less strong than those between fibroblasts, which could also be an indicator of their metastatic behaviour.

Using a method previously developed by the lab, the microparticles were reconstructed by analysing the stacks and the stain signals on their surface were identified. A method in MATLAB was developed which rescaled the signals of the two different cell types and compared them

in every position of the microparticle's surface. By doing this, the method was able to distinguish between the two cell types, as well as the existence of pure background coming from either stain, in an area of the microparticle's surface.

Before performing the newly developed method, the microparticles for which the fitting was not successful, either due to the extremely deformable shape of the microparticle or due to imaging issues (e.g. the microparticle was too large to fit in the z-stack or the microparticle was overexposed by the laser), were discarded. Some examples of these kind of microparticles can be seen in Figure 6.2 of the Supplementary figures. In the three repeats of the experiment, there were found particles with both cell types on their surface, with only one of the two stains, as well as with no cells touching their surface. An overview of the final amount of microparticles found for each case, after having discarded the unusable microparticles, can be seen in Figure 4.3.

To study the interactions between melanoma cells (MV3) and fibroblasts (SV80) and identify the forces they apply, we aimed on finding microparticles laying on the interface between the two cell types or simply interacting with both. In that way, the identification of the forces being applied by the two cell types during their interaction can be quantified. Finding microparticles on the interface between the two cell types was proven difficult, due to the random mixing of the microparticles with the cells during the seeding process. On the first experiment, 7 microparticles were found with both cell types attached to their surface. On the first repeat of the same experiment, only 1 microparticle able to be analysed was found having both cell types on its surface, while on the third experiment 11 microparticles appeared to have both stains (Figure 4.3). Since these are the microparticles of interest, the mean values of the stress fields, as calculated for their stains, were isolated for further analysis.

In Figure 4.4, an example of the results returned by the method, for a microparticle in the case where both cell types were found in its surface, is shown. The two stains are being displayed separately, with the green sphere corresponding to the MV3 cells and the red one to the SV80 cells. Firstly, the reduced signal of the stains is being displayed on the surface of the microparticle, in 3D and 2D. The largest signal values are displayed with white, while the darker areas correspond to less or no signals. Right below the first two spheres, the areas (white) where a cell is being identified are displayed. These are the results after comparing the reduced signals of the two cell types. The stress field was assigned to each cell type (Figure 4.4(c-d)) by matching the position of the stain's signal with the stress field in the same area of the microparticle's surface (Figures 4.4(e-f)).

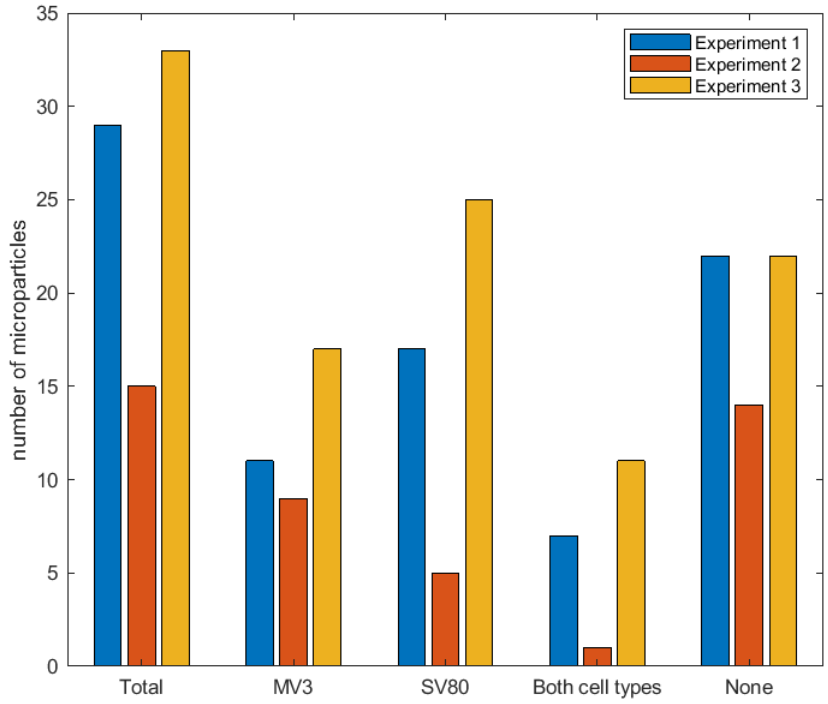

Figure 4.3: Histograms of the number of microparticles found with both, only one and none of the two cell types on their surface, for the three repeats of the experiment. *Number of microparticles found in each of the three cases* ***(a)*** *on the first experiment,* ***(b)*** *on the second experiment,* ***(c)*** *on the third and final experiment.*

Both normal and shear stress distributions for both cell types were found, and their mean values were calculated. In Figures 4.4(e-f), the complete normal and sheer stress applied on the same microparticle's surface, on which the two stains of Figures 4.4(a-b) were found, are displayed. This is the complete stress field, as it was found by looking at the deformations on the microparticle.

A boxplot of the mean values of the normal and shear stress field as calculated for the MV3 and SV80 cells, for the microparticles which had both cell types present on their surface, from all three experiments, can be seen in Figure 4.5. The same data in the form of a scatter, with the error bars being displayed, can be seen in Figures 6.3 of the Supplementary figures.

No significant results can be concluded from these data. The boxplot

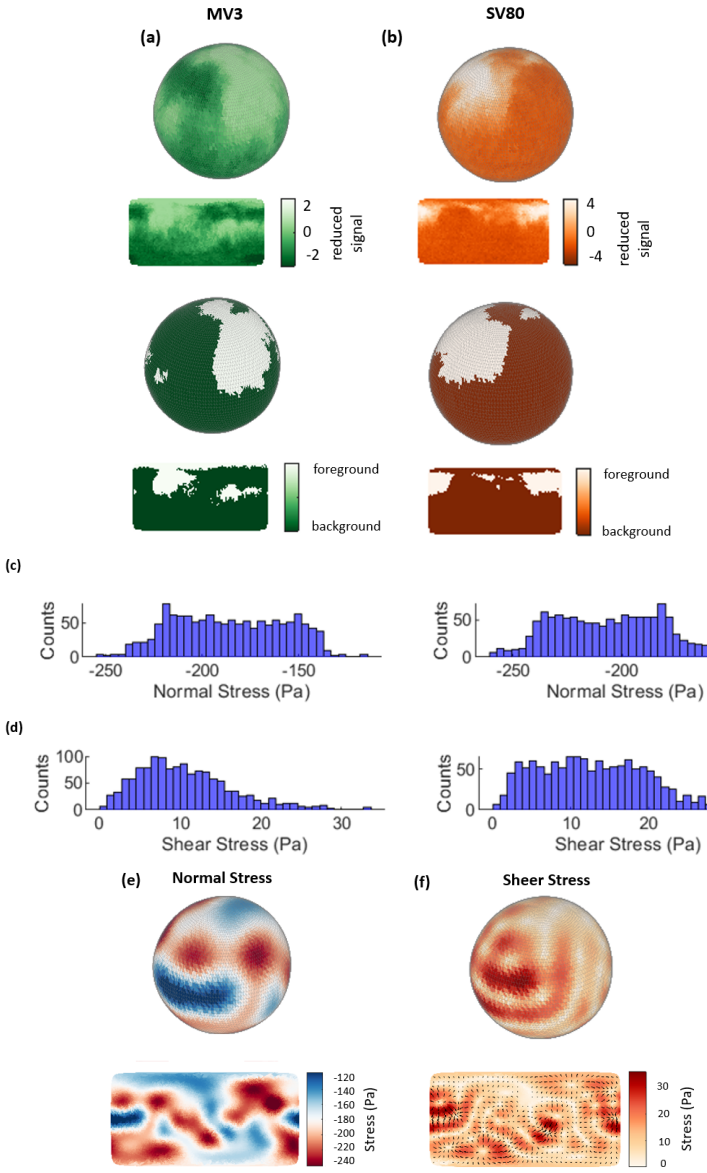

Figure 4.4: The results of the method for a microparticle with both cell types attached to its surface. ***(a-b)*** *The green sphere corresponds to the MV3 stain, while the red sphere to the SV80 stain. The white parts on the sphere show the position of the cell on the microparticle's surface. The first row of spheres is the stain reduced signal, while the second row shows the areas in which the method identifies the existence of a cell.* ***(c-d)*** *The stress fields distributions assigned to each of the two cell types.* ***(e-f)*** *The complete normal and sheer stress fields, on the same microparticle, respectively.*

of the first experiment (Figure 4.5(b)) shows that the MV3 cells displayed more lower negative mean values of normal stress than the SV80 cells. This indicated that the indentations formed due to the MV3 cells were larger and that they applied larger forces to the microparticle than the SV80 cells. However, this was not reproduced by the second repeat of the experiment (Figure 4.5(b)), in which the converse is true. In this case, the SV80 cells seemed to apply larger forces. This resulted in a complete absence of information when comparing the stress values of the two cell types, as it can be noted in Figure 4.5(a). In Figure 4.5(a), all the mean values for each type of stress, as calculated from all the microparticles with both stains found in all three experiments, are displayed. This holds for both normal and shear stress mean values, as well as their largest value when 95 % of the absolute data are taken into account. These results indicate that our experiments and analysis did not succeed into finding significant differences in the stress the two cell types apply, when interacting with one another.

As it can be noticed by looking at Figure 4.4(c-d) and Figure 6.3 of the Supplementary figures, the stress field distribution applied by the cells was very broad, resulting in a large standard deviation of the mean value. This indicates that the results displayed on the boxplots of Figure 4.5 are not accurate and the loss of information may be a consequence of that.

Further improvements of this experiment would include the acquisition of more data coming from microparticles which interact with both MV3 and SV80 cell types. It would also be interesting to examine the cases where the two cell types were seeded on a single-cell-type spheroid. That way, it could be determined if the similar stress distributions is a characteristic of the MV3-SV80 cell-cell interaction. Additionally, this experiment was performed by using the newly transducted MV3 eGFP LifeAct and SV80 mCherry LifeAct cells, which showed different behaviour when forming spheroids than other cell lines of the same cell types (MV3 YFP LifeAct, SV80 wild type), as shown in the following section. In accordance with these differences, the transduction may also have altered the way the two cell types interact. Attempts were made to use wild type MV3 and SV80 cell lines, but the staining methods, such as CellMask and CellTracker, did not give clear signal from the cells. The signal was not clear for the method to identify with accuracy the existence of one cell type over the other on the surface of the microparticle. This is what drove us to transduct the cell lines, as the LifeAct cell lines displayed a more distinguishable signal. If the wild type MV3 and SV80 cell lines are used, the resulted stress fields may be different.

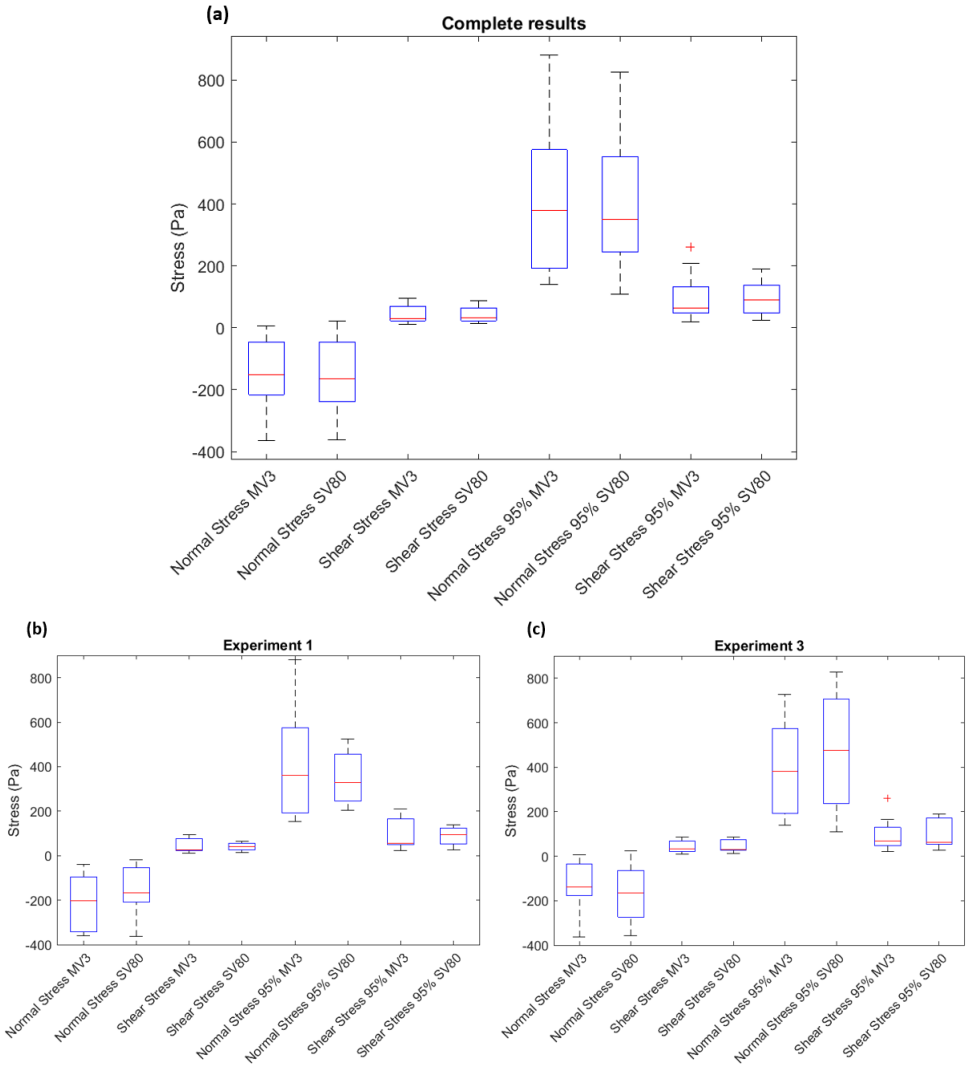

Figure 4.5: Stress values of the microparticles found interacting with both MV3 and SV80 cells do not show any significant difference between the two cell types. ***(a)*** *Boxplot of mean stress (normal and shear) values for all the microparticles from all three experiments.* ***(b)*** *Boxplot of the values of the 7 microparticles of experiment 1.* ***(c)*** *Boxplot of the values 11 microparticles found from experiment 3. No boxplot is shown for experiment 2 alone, since only 1 microparticle was found having both cell types attached to its surface.*

4.2 Phase separation of the two cell types

Melanoma MV3 cells and SV80 fibroblasts were seeded together in 3D spheroids, in different times and number conditions. The goal of this ex-

periment was to examine the mixing of the two cell types and investigate if they can display a sorting even when they are randomly intermixed.

4.2.1 Cell sorting of MV3 YFP LifeAct and wild type SV80 cells

For the first experiments, wild type SV80 cells stained with CellTracker Deep Red and MV3 YFP LifeAct cells were used. Initially, both cell types were seeded together at day 0 of the experiment. The result was a spheroid with a compact SV80 core and an MV3 ring around it, as shown in Figure 4.6(a). According to literature, the mixing of two cell types with different surface tensions results in a spheroid with the cell type of lower surface tension surrounding the cell type with the higher surface tension [5]. From this we can conclude that the MV3 have lower surface tension than the SV80 cells.

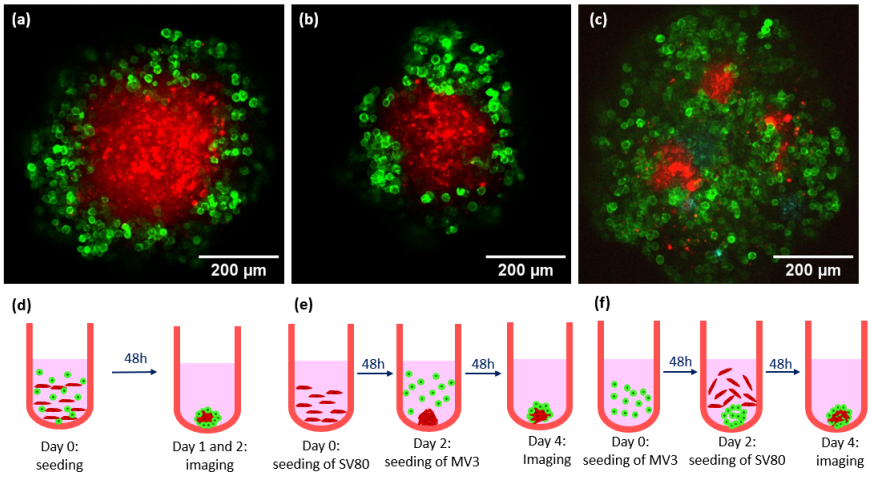

Figure 4.6: Seeding conditions of co-cultured spheroids influenced the final mixing of cells. ***(a)*** *A spheroid formed by seeding both MV3 and SV80 cells at day 0 of the experiment. A central core of SV80 was formed, surrounded by MV3.* ***(b)*** *A spheroid formed by seeding the SV80 at day 0 and the MV3 cells at day 2. Similarly, a core of SV80 is observed, with a ring of MV3 cells around it.* ***(c)*** *A spheroid formed by seeding the MV3 at day 0 and the SV80 cells at day 2. Small clusters of SV80 cells were found inside the MV3 spheroid. In every case, the spheroids were imaged 4 days after the initial seeding.* ***(d-f)*** *The seeding timelines of the three different experiments, shown in (a-c) respectively.*

A similar system, with hetero-spheroids formed from fibroblasts and cancer cells, was studied before by Yakavets *et al.* [15]. These studies

showed the same, with the cancer cells surrounding a core of fibroblasts. In this paper, the authors also seeded first the cancer cells and 2 days later a cell suspension of fibroblasts, in cell number ratios 1:1 and 1:3 (cancer cells:fibroblasts). These seeding conditions resulted in a more uniform spheroid, with small areas of fibroblasts inside a spherical structure of cancer cells, and not two completely separate areas of the two cell types. Expanding these findings, we seeded first the melanoma cells and 2 days later the fibroblasts in ratio 1:1, as well as the converse. Figure 4.6(b) shows a spheroid for which the fibroblasts (SV80) were seeded at day 0, while the melanoma (MV3) cells were seeded at day 2 of the experiment. The result was again similar to the first case, with a core of SV80 cells in the center of the spheroid, and the MV3 cells forming a ring around them. Figure 4.6(c) shows a spheroid where the opposite seeding conditions were used. The MV3 cells were seeded at day 0, while the SV80 cells were seeded 2 days later. In this case, the spheroid contained areas of SV80 cells inside the MV3 spherical structure, making the spheroid more mixed. In Figures 4.6(d-f) the schematic timelines of these three seeding conditions are displayed.

Next, by finding interesting the fact that Yakavets *et al.* [15] in their paper used the number ratio of 1:3, we decided to investigate the cases where the SV80 cells were seeded at day 2 in 5 different amounts, 1000, 3000, 6000, 8000 and 10000, corresponding to number ratios 1:1, 1:3, 1:6, 1:8 and 1:10. The results of the first experiment, for which these conditions were implemented, is shown in Figure 4.7.

Figures 4.7(a-b) show a 1:1 and 1:3 spheroid, with the MV3 having been seeded at day 0 and the SV80 at day 2. Both spheroids seemed to be more mixed, having multiple different areas of the two types of cells and not two giant separate areas as in the case of Figure 4.6(a). As the ratio increased from 1:3 to 1:6, the configuration of the cells changed. The spheroids being formed from ratios 1:6, 1:8 and 1:10 showed a complete separation between the two types of cells, as it can be seen in Figures 4.7(c-e). This indicated that there is a critical ratio between 1:3 and 1:6. Below this critical ratio the spheroid was more uniform, having multiple patches of the two types of cells, while above it the two cell lines showed a complete phase separation.

The 5 different number ratios, corresponding to spheroids being formed by 1000 MV3 cells and a range of 1000-10000 SV80 cells, were also investigated under the other two seeding-time conditions. The spheroids displayed in Figure 4.8 were formed by seeding the SV80 at day 0 and the MV3 at day 2. The result was a core of SV80 cells in the center of the spheroid, with a ring of MV3 around them, in every one of the 5 cases.

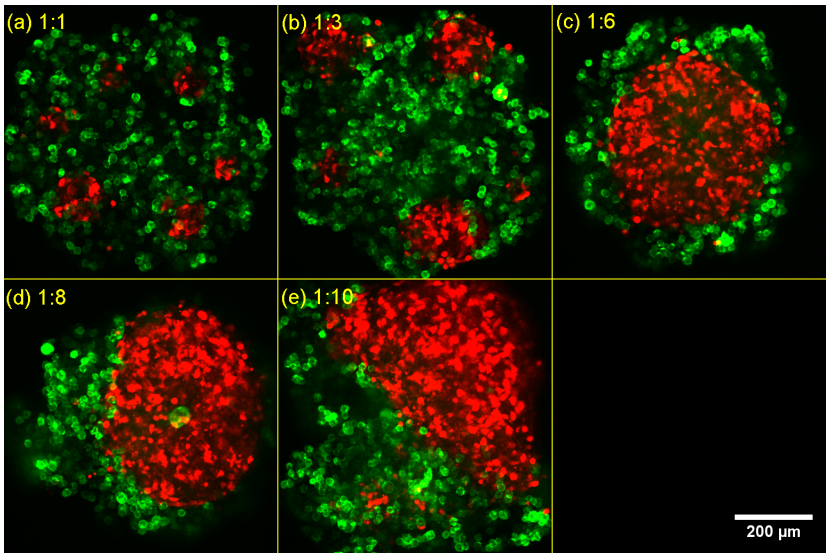

Figure 4.7: A critical number ratio between 1:3-1:6 appeared to induce complete separation of MV3 and SV80. *The MV3 cells were seeded at day 0 and the SV80 at day 2 in* ***(a)*** *1:1 number ratio,* ***(b)*** *1:3 number ratio,* ***(c)*** *1:6 number ratio,* ***(d)*** *1:8 number ratio and* ***(e)*** *1:10 number ratio. The number ratios correspond to MV3:SV80.*

Similar results were observed when both types of cells were seeded together at day 0, as shown in Figure 4.9.

4.2.2 Cell sorting of transducted MV3 eGFP LifeAct and SV80 mCherry LifeAct cells

To improve the signal of the cells and study their positions and configurations more accurately, MV3 and SV80 wild type cell lines were transducted into expressing eGFP and mCherry LifeAct. We know from the previous experiment that when the two types of cells were seeded together at day 0, or when the SV80 were seeded first and the MV3 were added 2 days later, a complete phase separation occured, regardless of the seeded number ratios. For this reason, we continued investigating the case where the MV3 cells were seeded at day 0 and the SV80 at day 2 of the experiment, using the transducted cell lines.

Firstly, the control conditions of the MV3 YFP LifeAct, the wild type SV80 stained with CellTracker Deep Red and the transducted cell lines, were compared. In these conditions, 1000 MV3 and 1000 SV80 cells were seeded separately. The resulted spheroids can be seen in Figure 4.10, where

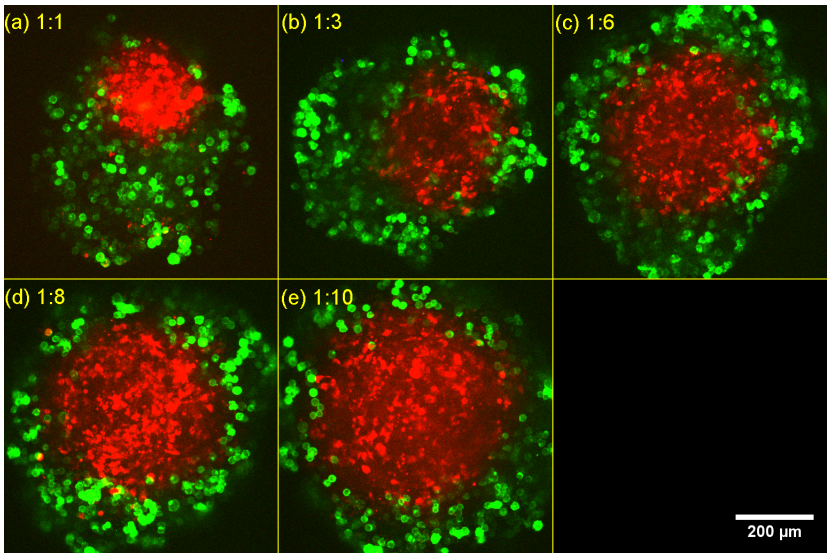

Figure 4.8: A central core of SV80 is formed, surrounded by MV3 cells, regardless of the number ratio, when the SV80 cells are seeded at day 0 and the MV3 at day 2. *A spheroid seeded at* ***(a)*** *1:1 number ratio,* ***(b)*** *1:3 number ratio,* ***(c)*** *1:6 number ratio,* ***(d)*** *1:8 number ratio and* ***(e)*** *1:10 number ratio. The number ratios correspond to ratio MV3:SV80.*

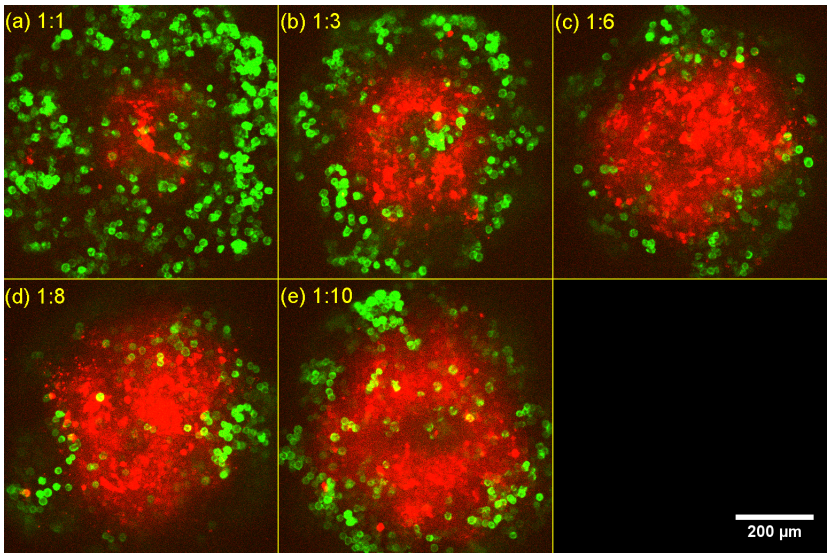

Figure 4.9: An SV80 core, with MV3 cells around it, is formed when the time-conditions cprrespond to seeding both cell types at day 0. *A spheroid seeded at* ***(a)*** *1:1 number ratio,* ***(b)*** *1:3 number ratio,* ***(c)*** *1:6 number ratio,* ***(d)*** *1:8 number ratio and* ***(e)*** *1:10 number ratio. The number ratios correspond to ratio MV3:SV80.*

both the fluorescent, as well as the BrightField images, are being shown. The differences between the spheroids formed by the newly transducted cells and the spheroids of the previous experiment are not very large, but still detectable. The spheroid of Figure 4.10(a,e), which was formed by the SV80 wild type cells stained with CellTracker Deep Red, was approximately 50 μm smaller than the one in Figure 4.10(b,f). Averaging over three spheroids, the SV80 wild type formed a spheroid of a diameter 295 ± 4.08 μm, while the SV80 mCherry LifeAct formed a spheroid of a diameter 358 ± 13.12 μm. In both cases, 1000 cells were seeded and the spheroids were grown for the same amount of time (4 days). Regarding the MV3 cells, the spheroids formed by the MV3 YFP LifeAct cells used in the previous experiments (Figure 4.10(c,g)) had approximately the same size as the ones formed by the new MV3 eGFP LifeAct cells (Figure 4.10(d,h)). The difference in this case is the fact that the MV3 eGFP LifeAct cells seemed to form a more compact core in the center with some more loose cells around it. This can be more easily observed by the BrightField image of the spheroid (Figure 4.10(h)). This core is not observed in the MV3 YFP LifeAct cells spheroid, which is more uniform (Figure 4.10(g)).

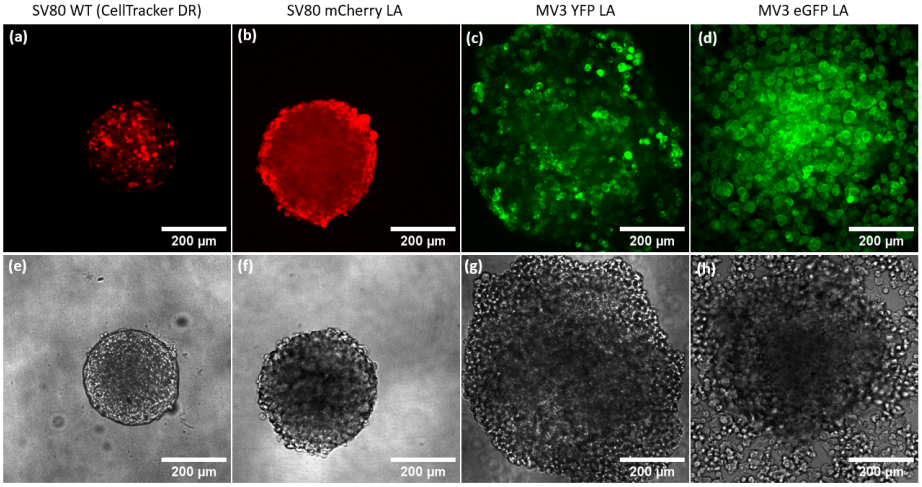

Figure 4.10: Spheroids formed by the WT SV80 cell line were more compact than the the SV80 mCherry LA spheroids. Spheroids formed by the MV3 eGFP LifeAct (LA) cell line seemed to form a more compact central core, something not observed in the case of MV3 YFP LifeAct (LA) cells. ***(a)*** *SV80 wild type stained with CellTracker Deep Red spheroid.* ***(b)*** *SV80 mCherry LifeAct spheroid.* ***(c)*** *MV3 YFP LifeAct spheroid.* ***(d)*** *MV3 eGFP LifeAct spheroid.* ***(e-h)*** *BrightField images of the same spheroids shown in (a-d) respectively.*

The same conditions as before were repeated for this experiment, using

the transducted MV3 and SV80 cell lines. The timeline of the experiment can be seen on Figure 4.6(f). 1000 melanoma MV3 cells were seeded at day 0, while SV80 cells in the range of 1000-10000 cells per well were seeded at day 2. This resulted in having 12 spheroids for each of the five number ratios (1:1, 1:3, 1:6, 1:8 and 1:10), and 12 spheroids for each of the three control conditions: MV3-only spheroids, SV80-only spheroids and MV3-SV80 hetero-spheroids with both cell types seeded at day 0. The spheroids were then imaged twice, at day 4 and day 7 of the experiment, to identify any changes in the mixing of the cells after the span of some days. The images were taken with a Confocal Spinning Disk, using a 10x objective. 3D stacks were acquired in a cube of approximately 700 x 700 x 8 μm^3, and their maximum projection was used, for a more clear signal. This experiment was repeated three times and the resulted images were analysed with a method written in MATLAB.

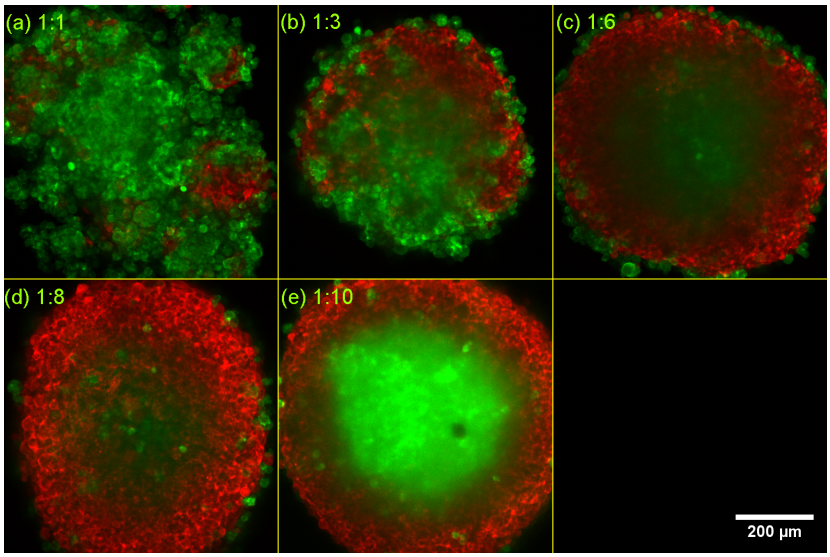

Figure 4.11: Spheroids formed by the transducted cell lines showed similar behavior for small number ratios, but oposite for larger ones, with the SV80 surrounding an MV3 core. *The MV3 cells were seeded at day 0 and SV80 at day 2 of the experiment. They were imaged at day 4 and seeded in* ***(a)*** *1:1 cell number ratio,* ***(b)*** *1:3 number ratio,* ***(c)*** *1:6 number ratio,* ***(d)*** *1:8 number ratio,* ***(e)*** *1:10 number ratio. The number ratios correspond to ratio MV3:SV80.*

Some indicative results from each of the 5 conditions can be seen in Figure 4.11. These spheroids were imaged at day 4 of the experiment. The spheroid in Figure 4.11(a), which corresponds to 1:1 ratio, looked similar with before. Patches of SV80 cells were found inside the MV3 structure. The rest number ratio conditions, however, appeared to be different.

The 1:3 spheroid (Figure 4.11(b)) did not have many SV80 patches inside the MV3 spherical structure. The SV80 cells showed a preference to cluster towards the edges of the spheroid. This became more evident in the larger number ratios, where the SV80 cells formed a ring-shaped structure around a core of MV3 cells (Figures 4.11(c-e)). A ratio between 1:3 and 1:6 remained a critical ratio, above which, in this case, the SV80 fully surrounded the MV3 cells. These results indicate that the transducted SV80 expressing mCherry have lower surface tension than the transducted MV3 cells expressing eGFP. This is the opposite result from the previous experiments, where wild type SV80 and MV3 YFP LifeAct cells were used.

To accurately determine the number of different areas of the two stains inside the spheroids for the 5 conditions, a method in MATLAB was written. The method, by using build-in functions, determined the amount of different areas, referred here as patches, each of the two cell types occupied. In Figure 4.12, the result returned by the method for one spheroid per condition is shown. Only the boundaries of the patches are displayed for visibility reasons. These spheroids belong to the first experiment performed by using the transducted cell lines. They were imaged at day 4 of the experiment, and the maximum projection of the 3D stack is displayed in the raw images. By finding the overlap area between the patches of the two stains, it was identified how many patches of one cell type were found inside a bigger area of the other cell type. The area each patch occupied, as well as their circularity, were also calculated. In Figure 4.12(a), a spheroid of the condition 1:1 is displayed. For this spheroid, the method identified 7 different SV80 patches with areas $0.12x10^5$ μm^2, $0.0262x10^5$ μm^2, $0.12x10^5$ μm^2, $0.44x10^5$ μm^2, $0.27x10^5$ μm^2 and $0.03x10^5$ μm^2. The area of the MV3 patch was calculated as $2.28x10^5$ μm^2. The spheroid in Figure 4.12(b) was formed by the 1:3 ratio condition. In this case one SV80 and two MV3 patches were identified, with areas $1.69x10^5$ μm^2 and $1.84x10^5$ μm^2, $0.06x10^5$ μm^2 respectively. The 1:6 ratio condition spheroid depicted in Figure 4.12(c) was found to have one SV80 patch with area $2.63x10^5$ μm^2 and five MV3 patches with areas $0.08x10^5$ μm^2, $0.06x10^5$ μm^2, $0.07x10^5$ μm^2, $1.73x10^5$ μm^2, and $0.04x10^5$ μm^2. Figure 4.12(d) shows a spheroid formed using the 1:8 ratio condition. For this spheroid, the method identified again one SV80 patch with area $2.95x10^5\mu m^2$ and 9 MV3 patches with areas $0.15x10^5$ μm^2, $0.32x10^5$ μm^2, $0.03x10^5\mu m^2$, $1.11x10^5$ μm^2, $0.04x10^5$ μm^2, $0.02x10^5$ μm^2, $0.16x10^5$ μm^2, $0.07x10^5\mu m^2$ and $0.05x10^5$ μm^2. Lastly, in Figure 4.12(e), a 1:10 spheroid is displayed. A single big area of 2.9812 was calculated for the SV80 cells. 11 MV3 patches were identified, with areas $0.07x10^5$ μm^2, $0.03x10^5$ μm^2, $0.02x10^5$ μm^2, $0.09x10^5$ μm^2, $0.03x10^5$ μm^2, $0.82x10^5$ μm^2, $0.02x10^5$ μm^2, $0.09x10^5\mu m^2$, $0.16x10^5$ μm^2, $0.11x10^5$ μm^2 and

$0.06x10^5\ \mu m^2$.

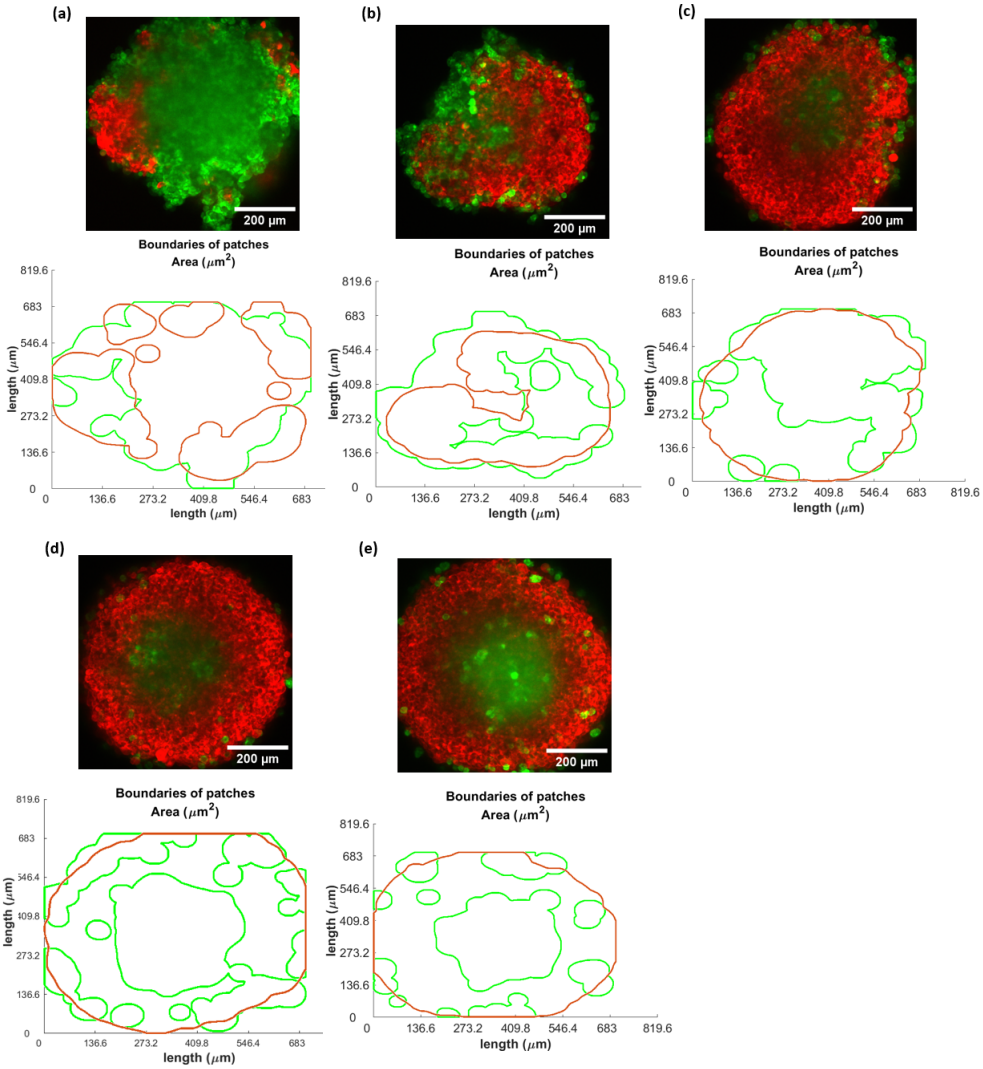

Figure 4.12: The developed method was able to identify the different patches of the two cell types. *Spheroids (from the first experiment, imaged at day 4) and their patches as found by the method displayed in µm, in ratio* ***(a)*** *1:1,* ***b*** *1:3,* ***(c)*** *1:6,* ***d*** *1:8 and* ***(e)*** *1:10. The SV80 cells are displayed in red, while the MV3 in green.*

For each of the five conditions, the method returned the average number of patches that belonged to the two stains, the average number of patches found to be inside the other stain and the average patch circularity and area they occupied. These statistics, for the first experiment, can be seen in Figure 4.13. In this figure panel, for every average value, its standard deviation in the form of error bar is displayed, indicating its

accuracy. For all three experiments, the images taken were first scanned for containing any flaws, making them unable to be used. The spheroids found to contain fibers, dust or any other dirt were discarded and not used for the analysis. After this process, there were approximately 10 (out of 12) spheroids left from each condition, for the first two experiments, while fewer for the third one.

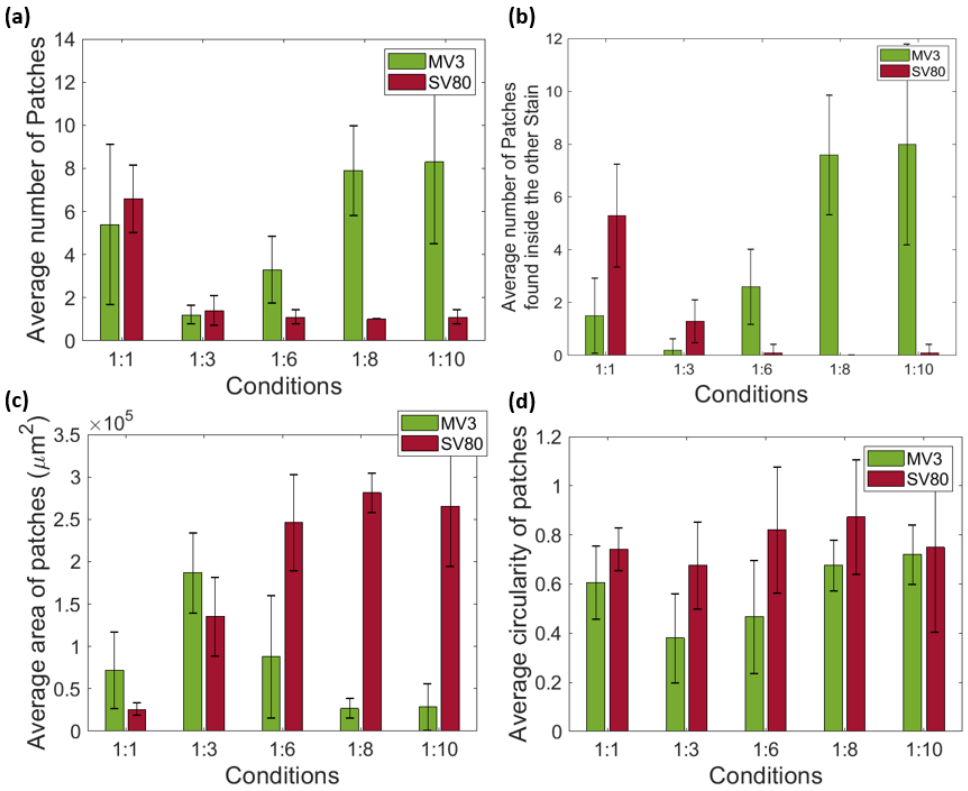

Figure 4.13: After 4 days of seeding, fewer and bigger SV80 patches, in contrast to more and smaller MV3 patches, appeared for increasing number ratios. ***(a)*** *Average number of patches of the two cell types, found in each of the five conditions.* ***(b)*** *Average number of patches of the stain indicated with the corresponding color found inside the other stain.* ***(c)*** *Average area the patches of each cell type occupied.* ***(d)*** *Average circularity of the patches. In all cases, the error bars of the calculations are shown.*

From Figure 4.13(a), it can be concluded that the amount of patches of the SV80 cells was larger in smaller number ratios. From the critical number ratio (between 1:3 and 1:6) and above, there was only one patch, something that can be also seen from Figure 4.12.

Figure 4.13(b) shows the average number of patches of each cell type

found inside the other cell type. At small ratios (1:1, 1:3) there were many SV80 patches included in areas where the MV3 cells were dominant. In large ratios, the situation was reversed, with many MV3 patches found in areas mostly occupied by the SV80 cells. This can be easily realized if one looks at Figure 4.12. For the ratio condition 1:10, there was one giant area of SV80 which formed a ring around the MV3 cells. This was identified by the method as the area of SV80 containing the MV3 core. Smaller patches of MV3 were found around this core, which are also identified as being inside the SV80 patch.

Figure 4.13(c) shows the average area the patches of the two cell types occupied, in μm^2. For the 1:1 ratio, both cell types were found to have patches occupying relatively small areas. This is because in this ratio the stains are divided in more patches than in the other ratios. Below the critical ratio, the MV3 patches were bigger, while above it, the SV80 patches were found to occupy a lot larger average area than the MV3. This is because in the large ratios, there is only one giant SV80 patch, while there are many small patches of MV3 cells. In terms of number of cells, we know from cell culture, that the MV3 cells were dividing twice as fast as the SV80 cells. From a proliferation assay, which is shown in Figure 6.6 of the Supplementary figures, the MV3 cells were doubling approximately every 24 hours. Since we seeded 1000 MV3 at day 0, 4 days later when the imaging took place, the total number of MV3 cells should be around 16000. For the ratios 1:1 and 1:3, 1000 and 3000 SV80 cells were seeded respectively, 2 days after the seeding of MV3. So at the day of imaging (day 4 of the experiment) the number of SV80 cells should be around 2000 and 6000 for these two conditions. Given these numbers, a small average area occupied by the SV80 patches compared to the MV3 ones was expected. The fact that the average area occupied by the MV3 is not 4 times larger than the SV80 is mainly because the MV3 are also divided in many patches (Figure 4.13(a)). For bigger ratios, the 6000, 8000 and 10000 SV80 cells doubled to 12000, 16000 and 20000 at day 4, making them comparable with the 16000 MV3 cells. However the area occupied by the SV80 is larger due to the fact that there is only one SV80 patch, while the MV3 cells are divided into many, as it can be seen in Figure 4.13(a).

Lastly, in Figure 4.13(d), the average circularity of the patches is shown. The deviations between the ratio conditions are not very large in this case. All patches seemed to be circular. The only observation is that in every case, the SV80 cells form more circular patches. This does not come as a surprise, since when the two cell types were seeded alone, the SV80 cells formed a more compact and circular spheroid, than the MV3 cells (Figure 4.10).

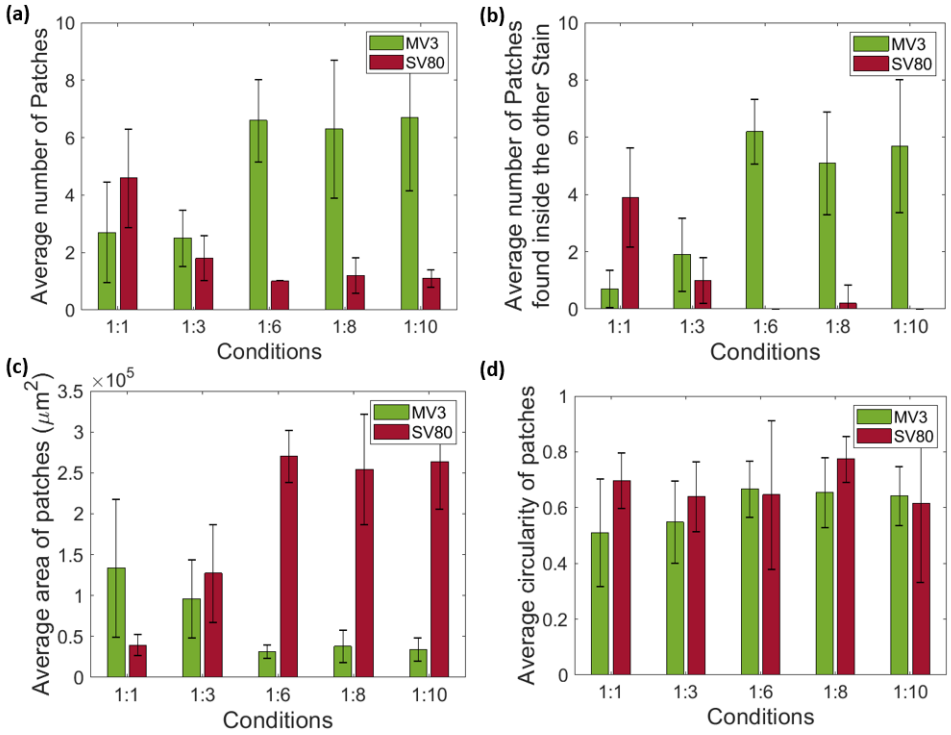

Figure 4.14: 7 days after seeding, a decrease in the number of clusters for both cell types was observed, with a simultaneous increase of the clusters' average size, in small number ratios. ***(a)*** *Average number of patches of the two cell types, for each of the five conditions, at day 7.* ***(b)*** *Average number of patches of the stain indicated with the corresponding color found inside the other stain.* ***(c)*** *Average area the patches of each cell type occupied.* ***(d)*** *Average circularity of the patches. The error bars for each case are shown.*

In Figure 4.14, the same statistics, for the same spheroids, as imaged at day 7 are shown. Figure 4.14(a) shows the average number of patches in the spheroids. Comparing this figure with Figure 4.13(a), which corresponds to the images taken at day 4, one can see that in most cases the average number of patches, both for the MV3 and the SV80 cells, showed a small decrease. As the spheroids grow and the cells differentiate, the smaller clusters of cells tend to merge into bigger ones. This is one of the phenomena that have been observed before [6], which the cell types used in this project obeyed. The only cases where this observation was not proven, was for the MV3 cells in the ratios 1:3 and 1:6, for which the average number of patches increased. This can be understood if one thinks about the fact that we were close to the critical ratio, where the changes are more dramatic. As the SV80 patches take different pathways to merge into

a single giant one, the MV3 patches were being split temporarily, resulting into an increase in the number of patches. A complete phase separation, especially for the small number ratio conditions, did not occur during the 7 days the experiment took place. Although the the decrease in the number of clusters was observable, the p-values of the distributions should be calculated, to establish whether the difference is significant.

Figure 4.14(b) shows the patches of the two stains found inside the other one. For the 1:1 ratio, the SV80 patches found inside the MV3 ones were still more in number. Similarly with before (Figure 4.13), for the ratios 1:8 and 1:10, there were many MV3 patches found inside the SV80. Again, a more dramatic change is found close to the critical ratio. For the 1:3 condition, after 7 days, the average number of MV3 patches found inside the SV80 ones was larger, in contrast to when the exact same spheroids were monitored at day 4 of the experiment. During the latter, the average number of SV80 patches was found to be larger (Figure 4.13(b)). For the 1:6 ratio, the average number of MV3 patches inside the SV80 increased, again as a consequence to the merging of the SV80 patches.

In Figure 4.14(c), the average number of area occupied by the patches is displayed. Comparing it with Figure 4.13(c), the differences occurred mostly at small ratios. For both cell types, the average area of the patches increased for the ratio condition 1:1, since many small patches merged to bigger ones. For the ratios 1:3 an 1:6, the average area for the MV3 patches decreased. Since the cells are dividing, the size of the patches should increase. The fact that their average area decreased by this considerate amount reflects the fact that the patches broke to smaller ones.

Lastly, Figure 4.14(d) shows the circularity of the patches after 7 days. The values are similar to those found before (Figure 4.13(d)).

All the above results were found and analysed for the first experiment. The exact same conditions were repeated two times, in which similar results were reproduced. These results can be seen in Figures 6.7-6.10 of the Supplementary figures. In Figure 6.4 of the Supplementary figures, the statistics of the experiment where the wild type SV80 and MV3 YFP LifeAct cells were used for forming spheroids. This experiment was only done once, with 3 spheroids being imaged at day 3 of the experiment. The number of samples was low, but even the spheroids formed entirely out of one of the two cell types (Figure 4.10) showed that there were differences between the two systems. The two experimental systems showed almost opposite results, with the MV3 showing lower surface tension in the first case, while the SV80 cells in the second one. This change in behaviour may be a result of the transduction of the cells. When the cells are transfected, it cannot be known where inside the cell's DNA the viral DNA ends up

and how, or if, it affects the behaviour of the cells.

Further experiments could include the comparison of the cell's clustering, more than one week after the beginning of the experiment. By tracking the changes of the cells' mixing for longer periods, it could be determined if different initial conditions of the two cell types would still lead to a complete phase separation with the exact same configuration. Additionally, the reversed seeding-time conditions could also be examined, with the SV80 cells being seeded forst, followed by MV3 cells 2 days later. One attempt of this experiment, for a ratio condition 1:1 can be seen in Figure 6.11 of the Supplementary figures. One could track the changes between the two different seeding-time conditions and investigate if the two final configurations will be the same and if so, if the time required for the two systems to reach the final configuration will be the same. Lastly, by observing the fact that the cells have properties resembling them to liquids [5, 6], one could examine the angle of the interface between the two cell types, when they are completely separated. In Figure 6.12 of the Supplementary figures, a spheroid formed entirely out of SV80 mCherry LifeAct and one out of MV3 eGFP LifeAct before they merge is shown. The two spheroids were grown for a week before the image was taken. The spheroids did not merge instantly, but they rather resemble two oil droplets, with a certain angle between them. The two spheroids are round with a clear interface between them. Given this result, an interesting continuation would be to investigate the merging of the spheroids over a longer period of time and identify if the cells will again reach the same configuration as when they are seeded together as single cells. As this process occurs, the change in angle between the two spheroids could be calculated. On top of that, one could also embed microparticles, to study the interaction forces as the two spheroids fuse.

Chapter 5

Conclusions

The new method successfully managed to quantitatively compare the signals of two different cell types (MV3 and SV80) and identify which cell type is found in a specific area on the deformable microparticle's surface. By calculating the stress field applied in the microparticles, the stress fields applied by the two cell types were found. Only microparticles which were found to interact with both cell types were considered. The mean values of the normal and shear stress distributions, as well as the largest value when taking into account 95 % of the data for the absolute normal and shear stress fields, were calculated for both cell types. The results showed that there was no significant difference, within the measurement accuracy, between these values for the two cell lines. Given this outcome, we were not able to identify whether one cell type is applying larger forces than the other one, during their interaction.

Furthermore, by randomly mixing the two cell types in 3D cultures, it was shown that they tend to cluster and form two separate areas. By seeding first the MV3 and two days later the SV80 cells, in different number ratio (MV3:SV80) conditions, we examined whether the cells reached the same final configuration even when starting with different initial conditions. For small number ratios, a small decrease in the number of clusters for both cell types, with a simultaneous increase of the average cluster-size. This could mean that smaller clusters merged into larger ones. However, in the duration of one week no complete phase separation was observed. In contrast, for large number ratios, the cells were almost completely separated by day 4 of the experiment. There was found that a critical number ratio exists between 1:3 and 1:6 (MV3:SV80), above which the two types of cells displayed a complete phase separation. This experiment was performed in two different systems. When SV80 wild type and

MV3 YFP LifeAct cells were used, the MV3 tend to form a ring around the SV80, showing that the MV3 cell line had lower surface tension than the SV80 cell line. The opposite was observed when the transducted cell lines (MV3 eGFP LifeAct and SV80 YFP LifeAct) were used. In this case, it was observed that the SV80 tend to surround the MV3 cells, indicating that the SV80 are the ones with lower surface tension.

Acknowledgements

I would like to express my gratitude towards Rick Rodrigues de Mercado for the invaluable guidance and feedback throughout the project. I would like thank Prof. Dr. Thomas Schmidt for giving me the opportunity to do this project. Many thanks to Julia Eckert and Esmée Adegeest for their support. Lastly, special thanks to Andreea Iosif for her assistance and for taking the time to create the transducted cell lines for my project.

Chapter 6

Supplementary figures

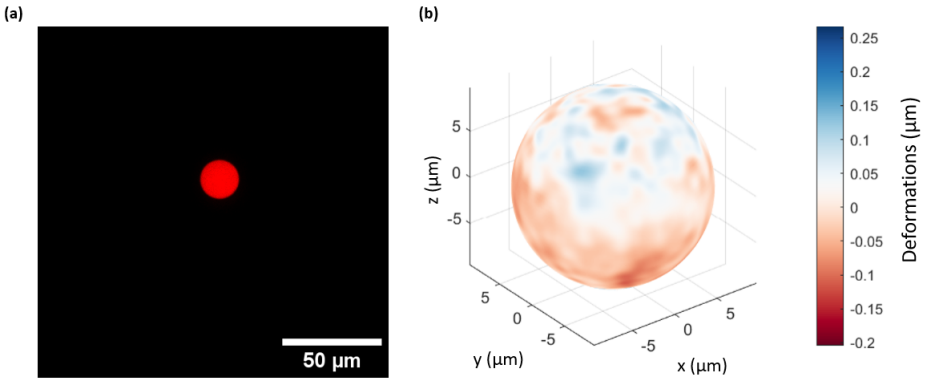

Figure 6.1: Test reconstruction of a soft hydrogel microparticle before using the functionalized and labeled sample for the experiments. ***(a)*** *Raw image of the microparticle.* ***(b)*** *The microparticle's shape after performing the first analysis.*

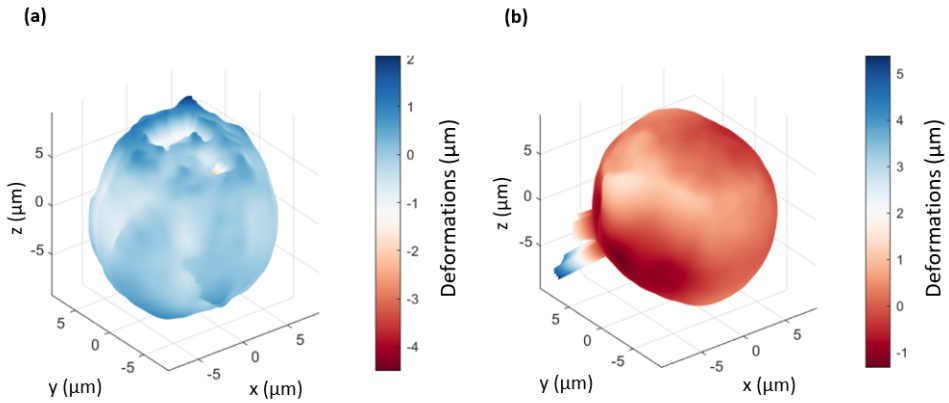

Figure 6.2: Two examples of microparticles which could not be used. ***(a)*** *A microparticle displaying a hole on the upper part of its surface.* ***(b)*** *A microparticle with spikes. The reasons for the inaccurate reconstruction of these microparticles may include their overexposion during imaging, due to their size may not had been able to fit in the field of view or two or more microparticles were touching each other, resulting in an abnormal reconstruction of the sphere.*

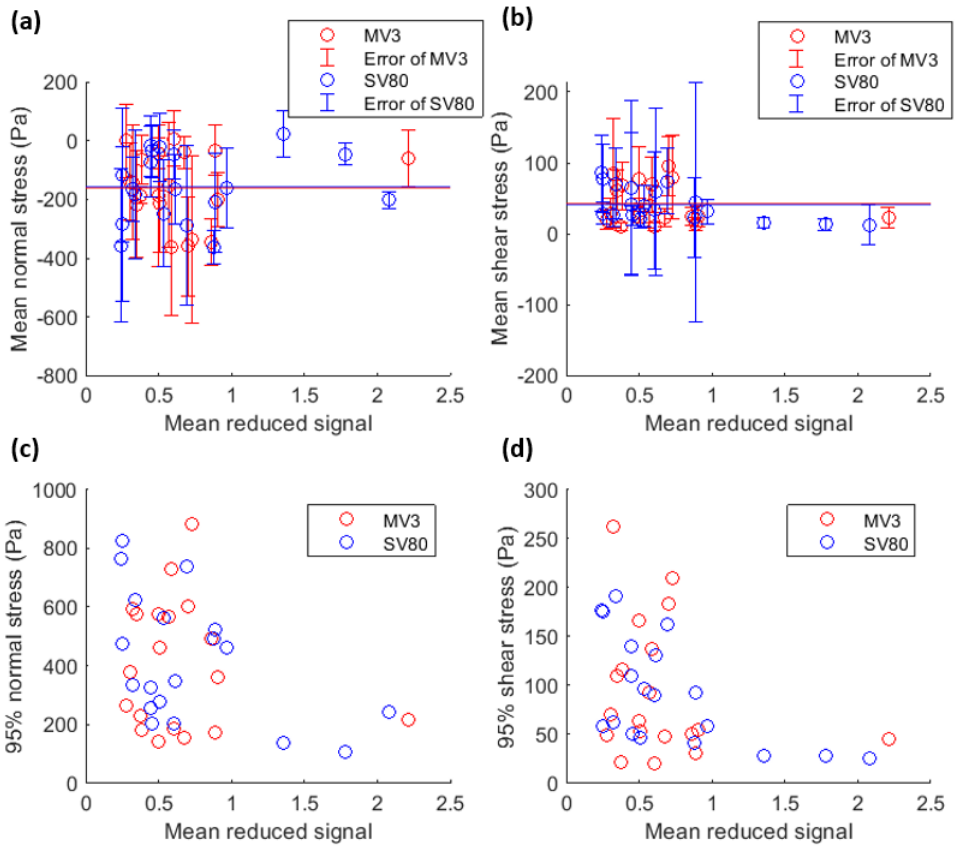

Figure 6.3: The mean stress values of the two cell types, as calculated for the microparticles appearing to have both stains on their surface, versus the reduced signal of the cells, in a scatter form. ***(a)*** *The mean normal stress values for all the microparticles. The MV3 cells' values are displayed in red, while the SV80's in blue. The standard deviation for each value is also displayed in the corresponding color, as an error bar. The two horizontal lines correspond to the mean values for the two different stains, as calculated from the values of all the microparticles.* ***(b)*** *The mean shear stress values.* ***(c)*** *The largest normal stress values taking into account 95 % of the absolute data.* ***(d)*** *The largest shear stress values taking into account 95 % of the absolute data.*

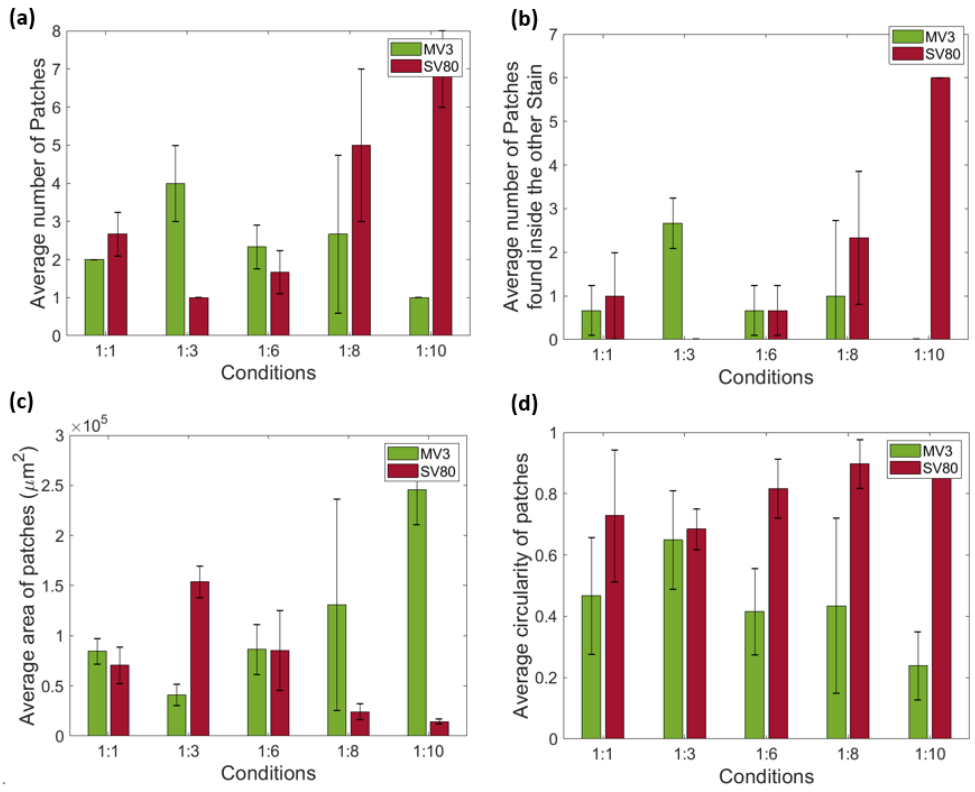

Figure 6.4: Statistics of the patches for the SV80 wild type and MV3 YFP LifeAct cells as returned by the method. The MV3 cells were seeded at day 0 and the SV80 at day 2. The imaging took place at day 3 of the experiment. The number of spheroids analysed were 3 per ratio condition. ***(a)*** *The average number of patches for the two cell types, as calculated for the 5 different ratio conditions.* ***(b)*** *The average number of patches of one stain found inside the other stain.* ***(c)*** *The average number of area the patches of each cell type occupy, in* μm^2. ***(d)*** *The average circularity of the patches.*

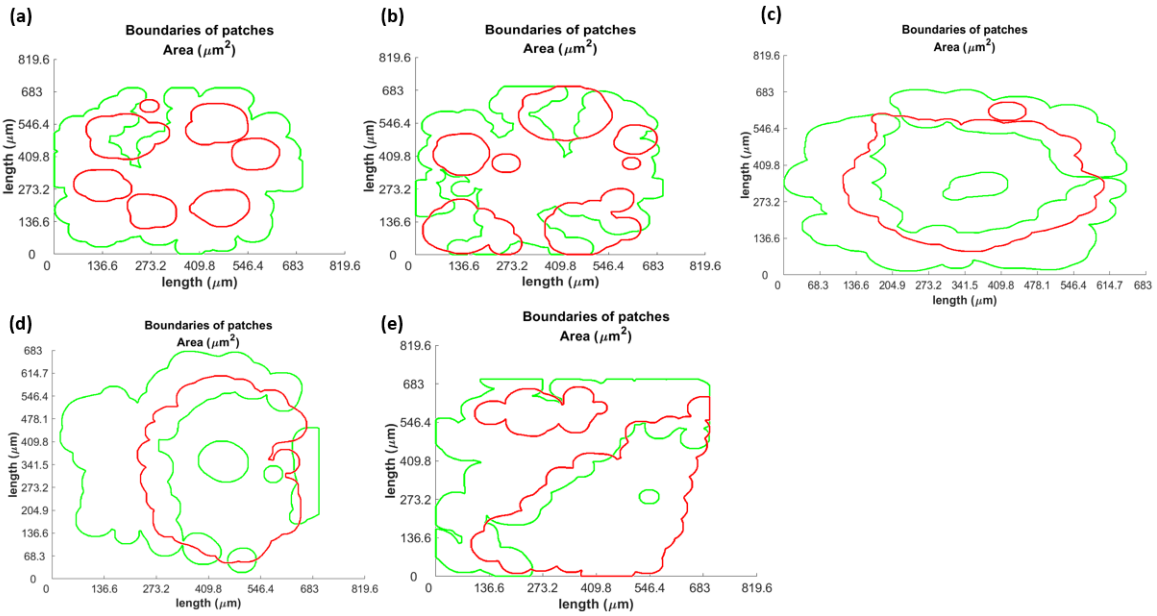

Figure 6.5: The boundaries of the patches of the spheroids depicted in Figured 17, as found by the method. These are the spheroids formed by using the SV80 wild type and MV3 YFP LifeAct cells, with the MV3 being seeded at day 0, the SV80 at day 2 and imaged at day 3. ***(a)*** *1:1 ratio, corresponding to the spheroid in Figure 17(a).* ***(b)*** *1:3 ratio, corresponding to the spheroid in Figure 17(b).* ***(c)*** *1:6 ratio, corresponding to the spheroid in Figure 17(c).* ***(d)*** *1:8 ratio, corresponding to the spheroid in Figure 17(d).* ***(e)*** *1:10 ratio, corresponding to the spheroid in Figure 17(e).*

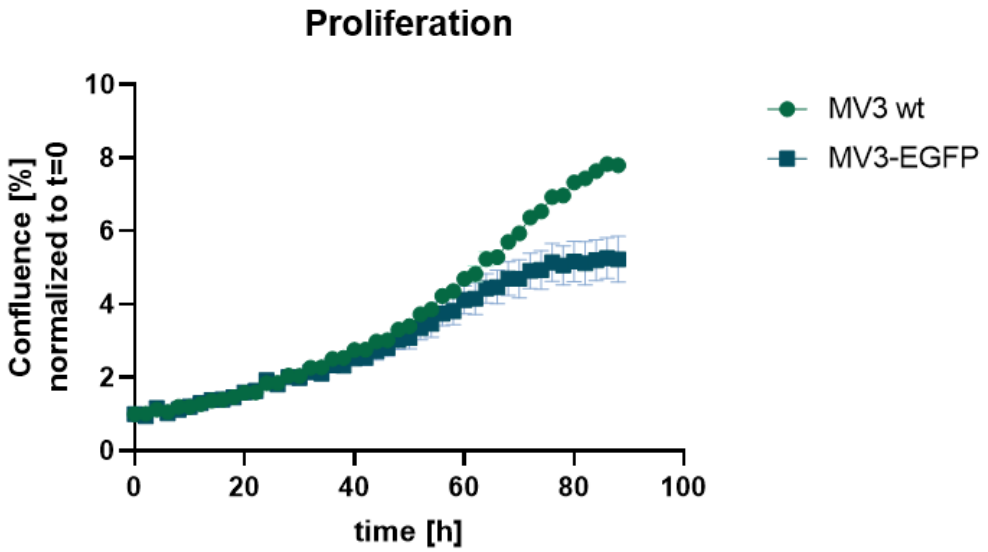

Figure 6.6: Proliferation assay performed on the MV3 wild type and MV3 eGFP LifeAct cells lines. *Both cell lines are doubling in population every approximately 24 hours. After around three days, the MV3 eGFP LifeAct seemed to not proliferate as fast as the MV3 wild type, something typically observed in transducted cell lines.*

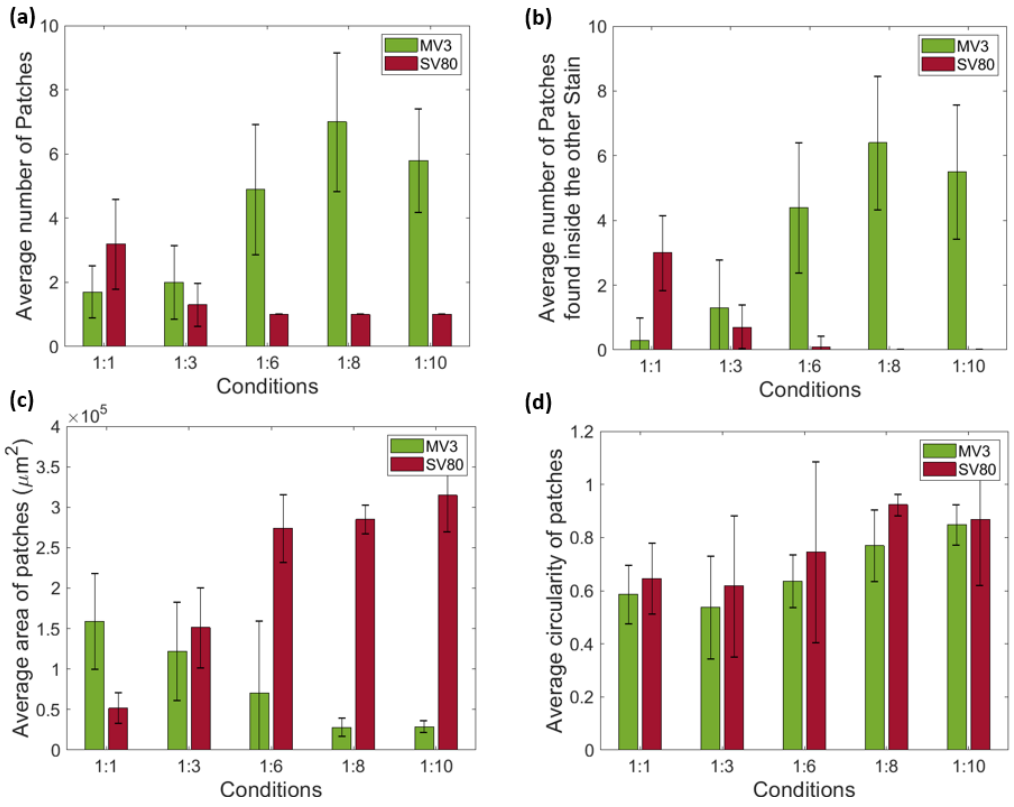

Figure 6.7: Statistics of the patches from the second experiment performed by using the SV80 mCherry LifeAct and MV3 eGFP LifeAct cells, imaged at day 4. The results are very similar to the ones from the first experiment. *The MV3 cells were seeded at day 0 and the SV80 at day 2. The number of spheroids analysed were 10 per ratio condition.* ***(a)*** *The average number of patches for the two cell types, as calculated for the 5 different ratio conditions.* ***(b)*** *The average number of patches of one stain found inside the other stain.* ***(c)*** *The average number of area the patches of each cell type occupy, in μm^2.* ***(d)*** *The average circularity of the patches.*

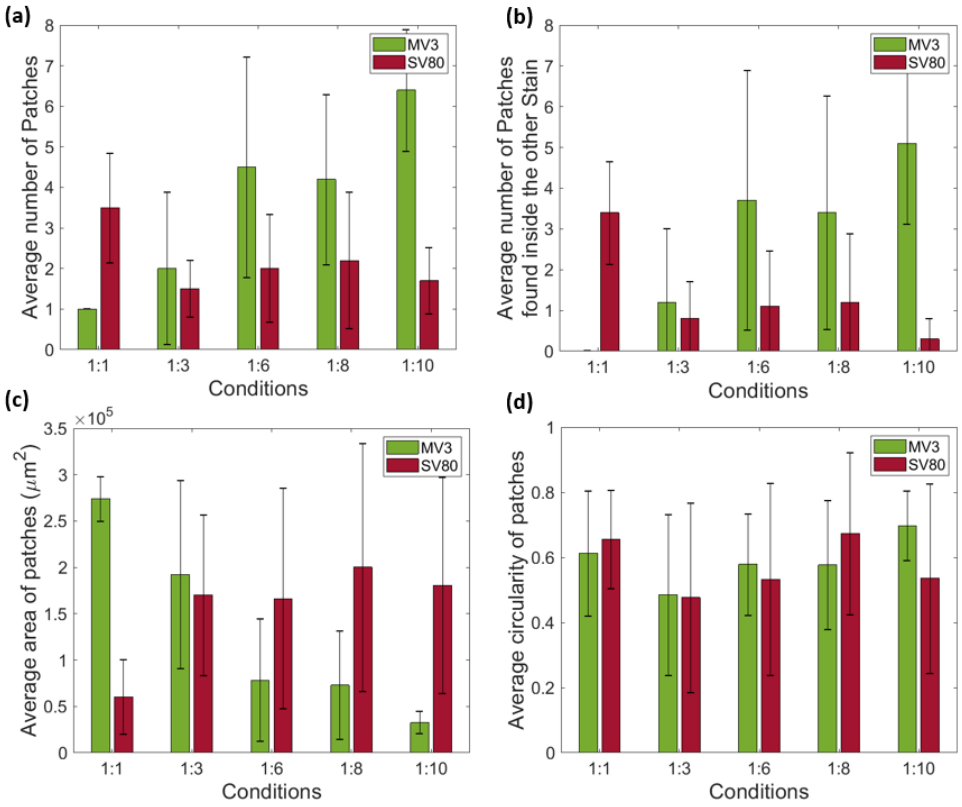

Figure 6.8: Statistics of the patches from the second experiment performed by using the SV80 mCherry LifeAct and MV3 eGFP LifeAct cells, imaged at day 7. *The MV3 cells were seeded at day 0 and the SV80 at day 2. The number of spheroids analysed were 10 per ratio condition.* ***(a)*** *The average number of patches for the two cell types, as calculated for the 5 different ratio conditions.* ***(b)*** *The average number of patches of one stain found inside the other stain.* ***(c)*** *The average number of area the patches of each cell type occupy, in μm^2.* ***(d)*** *The average circularity of the patches.*

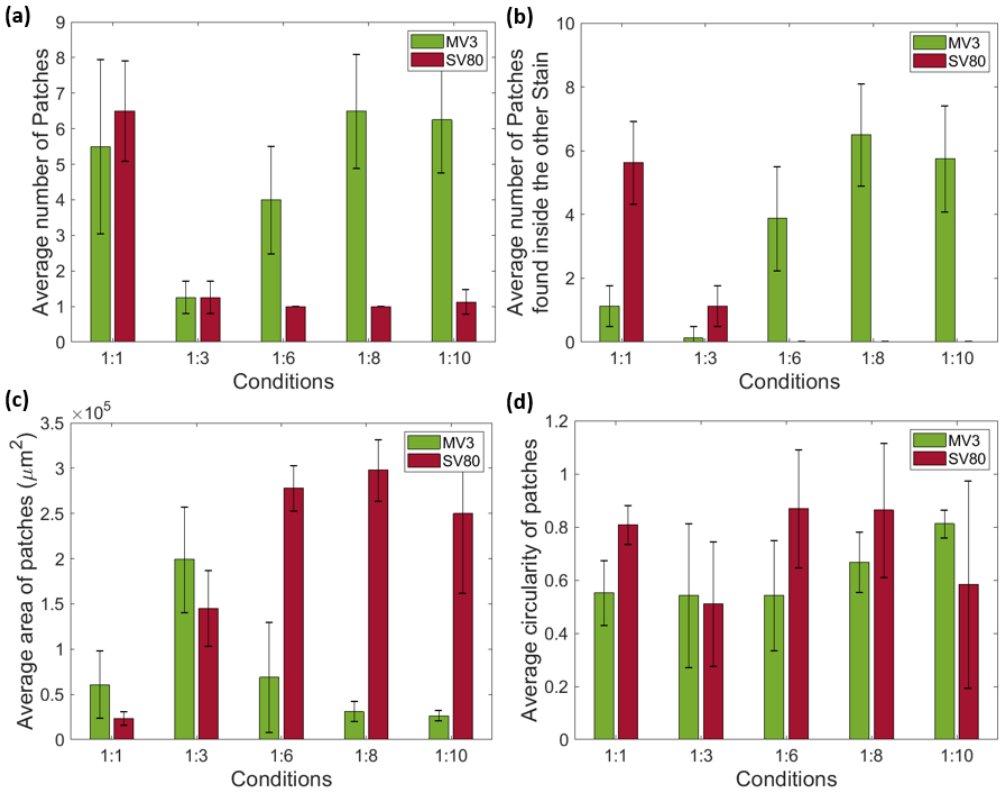

Figure 6.9: Statistics of the patches from the third experiment performed by using the SV80 mCherry LifeAct and MV3 eGFP LifeAct cells, imaged at day 4. *The MV3 cells were seeded at day 0 and the SV80 at day 2. The number of spheroids analysed were 8 per ratio condition.* ***(a)*** *The average number of patches for the two cell types, as calculated for the 5 different ratio conditions.* ***(b)*** *The average number of patches of one stain found inside the other stain.* ***(c)*** *The average number of area the patches of each cell type occupy, in* μm^2. ***(d)*** *The average circularity of the patches.*

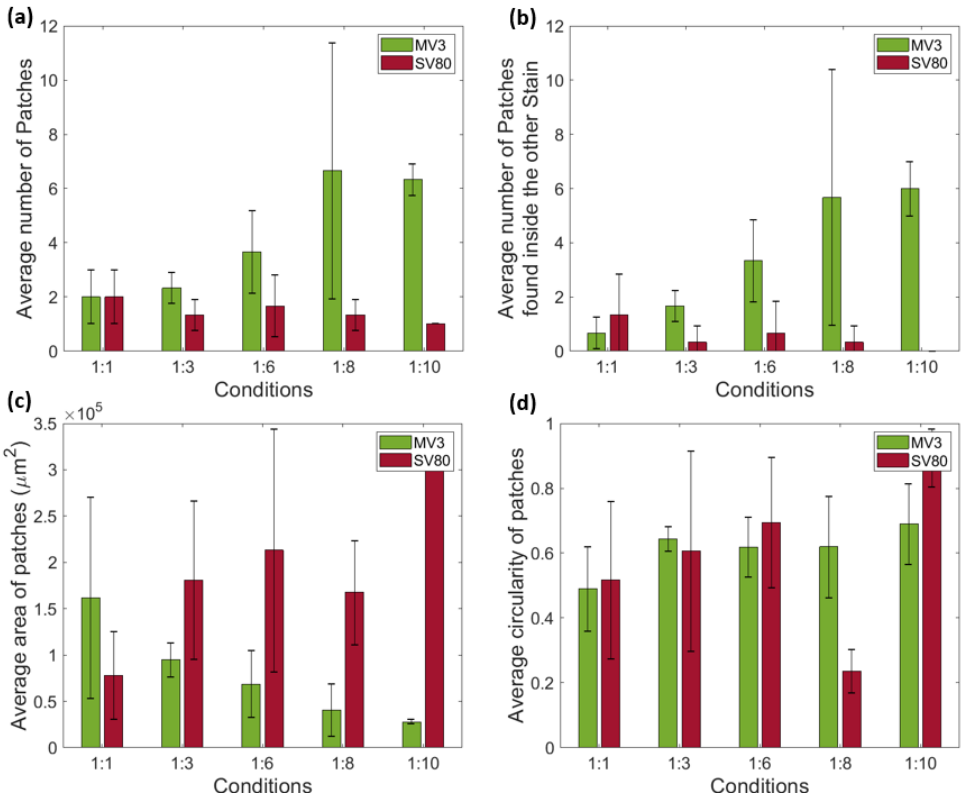

Figure 6.10: Statistics of the patches from the third experiment performed by using the SV80 mCherry LifeAct and MV3 eGFP LifeAct cells, imaged at day 7. *The MV3 cells were seeded at day 0 and the SV80 at day 2. The number of spheroids analysed were 3 per ratio condition, due to loss of clean samples during the medium refreshing.* ***(a)*** *The average number of patches for the two cell types, as calculated for the 5 different ratio conditions.* ***(b)*** *The average number of patches of one stain found inside the other stain.* ***(c)*** *The average number of area the patches of each cell type occupy, in μm^2.* ***(d)*** *The average circularity of the patches.*

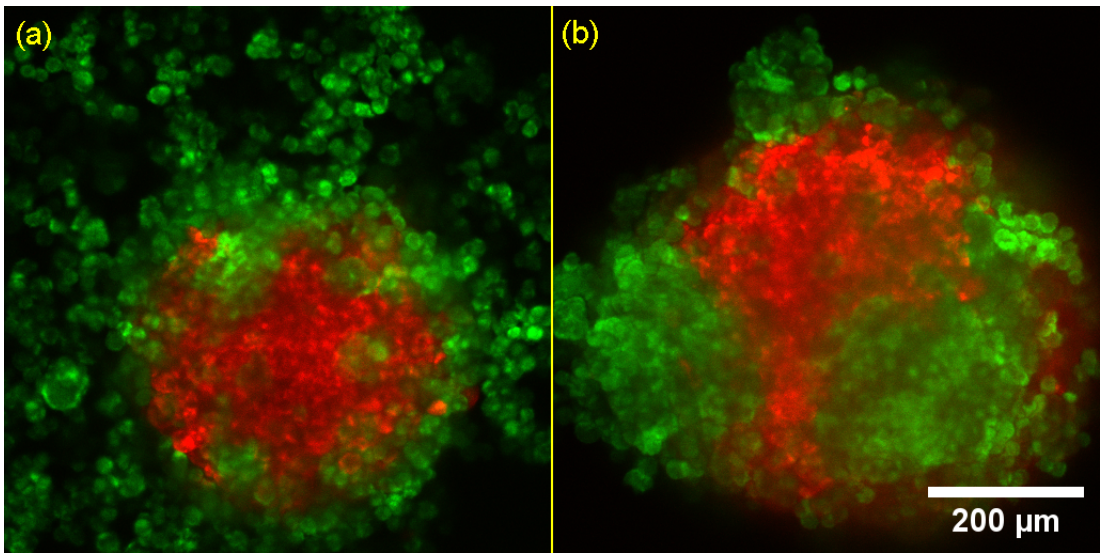

Figure 6.11: An example spheroid, formed by the SV80 mCherry LifeAct and MV3 eGFP LifeAct cell lines. *The SV80 were seeded at day 0 and the MV3 cells at day 2.* ***(a)*** *Imaged at day 4* ***(b)*** *Imaged at day 7. After a period of 7 days, the MV3 cells seemed to cluster and move towards the center of the SV80 spheroid.*

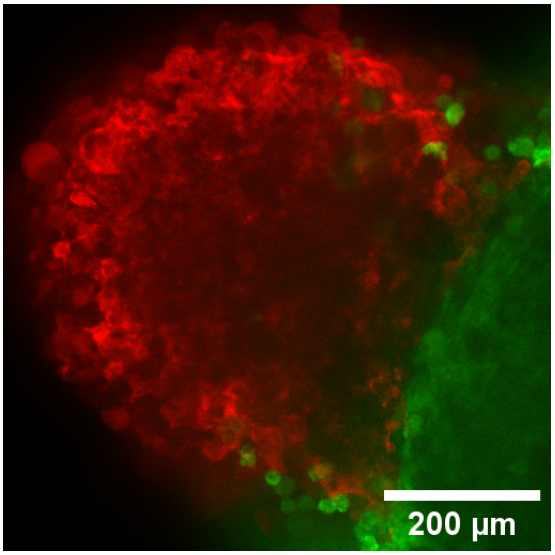

Figure 6.12: An MV3 eGFP LifeAct spheroid (green) and SV80 mCherry LifeAct spheroid fusion. *The spheroids were grown for 7 days. At day 7, the spheroids were transferred in the same seeding well. The imaging took place at day 8 of the experiment. The spheroids did not completely mix instantly, they rather seem like two oil droplets, with a certain interface angle.*

Bibliography

[1] L. A. Kunz-Schughart, J. P. Freyer, F. Hofstaedter, and R. Ebner, *The use of 3-D cultures for high-throughput screening: the multicellular spheroid model*, J Biomol Screen **9**, 273 (2004).

[2] F. Hirschhaeuser, H. Menne, C. Dittfeld, J. West, W. Mueller-Klieser, and L. A. Kunz-Schughart, *Multicellular tumor spheroids: an underestimated tool is catching up again*, J Biotechnol **148**, 3 (2010).

[3] N. Nishida-Aoki and T. S. Gujral, *Emerging approaches to study cell-cell interactions in tumor microenvironment*, Oncotarget **10**, 785 (2019).

[4] D. Yip and C. H. Cho, *A multicellular 3D heterospheroid model of liver tumor and stromal cells in collagen gel for anti-cancer drug testing*, Biochem Biophys Res Commun **433**, 327 (2013).

[5] R. A. Foty, C. M. Pfleger, G. Forgacs, and M. S. Steinberg, *Surface tensions of embryonic tissues predict their mutual envelopment behavior*, Development **122**, 1611 (1996).

[6] M. S. Steinberg and M. Takeichi, *Experimental specification of cell sorting, tissue spreading, and specific spatial patterning by quantitative differences in cadherin expression*, Proc Natl Acad Sci U S A **91**, 206 (1994).

[7] D. Vorselen, Y. Wang, M. M. de Jesus, P. K. Shah, M. J. Footer, M. Huse, W. Cai, and J. A. Theriot, *Microparticle traction force microscopy reveals subcellular force exertion patterns in immune cell–target interactions*, Nature Communications **11**, 20 (2020).

[8] D. Tsvirkun, J. Revilloud, A. Giannetti, and C. Verdier, *The intriguing role of collagen on the rheology of cancer cell spheroids*, Journal of Biomechanics **141**, 111229 (2022).

[9] A. Blumlein, N. Williams, and J. J. McManus, *The mechanical properties of individual cell spheroids*, Scientific Reports **7**, 7346 (2017).

[10] R. A. Gutierrez, W. Fang, H. Kesari, and E. M. Darling, *Force sensors for measuring microenvironmental forces during mesenchymal condensation*, Biomaterials **270**, 120684 (2021).

[11] A. H. Shain and B. C. Bastian, *From melanocytes to melanomas*, Nature Reviews Cancer **16**, 345 (2016).

[12] M. L. Manning, R. A. Foty, M. S. Steinberg, and E.-M. Schoetz, *Coaction of intercellular adhesion and cortical tension specifies tissue surface tension*, Proceedings of the National Academy of Sciences **107**, 12517 (2010).

[13] V. P. Skripov and A. V. Skripov, *Spinodal decomposition (phase transitions via unstable states)*, Soviet Physics Uspekhi **22**, 389 (1979).

[14] Z. Hiroi, H. Hayamizu, T. Yoshida, Y. Muraoka, Y. Okamoto, J.-i. Yamaura, and Y. Ueda, *Spinodal Decomposition in the TiO2–VO2 System*, Chemistry of Materials **25**, 2202 (2013).

[15] I. Yakavets, A. Francois, A. Benoit, J.-L. Merlin, L. Bezdetnaya, and G. Vogin, *Advanced co-culture 3D breast cancer model for investigation of fibrosis induced by external stimuli: optimization study*, Scientific Reports **10**, 21273 (2020).

[16] T. K. Kim and J. H. Eberwine, *Mammalian cell transfection: the present and the future*, Analytical and Bioanalytical Chemistry **397**, 3173 (2010).

[17] A. A. Sane, *Characterising 3D Force Sensors to Study Cellular Forces in Tissues*, MSc Thesis, Leiden University (2021).

[18] M. Janiszewska, M. C. Primi, and T. Izard, *Cell adhesion in cancer: Beyond the migration of single cells*, J Biol Chem **295**, 2495 (2020).